Odoribacter splanchnicus mitigates pathogen-induced gut inflammation and its associated pathogenesis via its secreted bacteriocin

Dipasree Hajra[1^], Debapriya Mukherjee [1#], Rhea Vij [1#], Raju S Rajmani [2], Venkatareddy Dadireddy[3], Deepakash Das[4], Tanweer Hussain[4], Mahipal Ganji[3], Utpal Tatu [3], Dipshikha Chakravortty [1,5 *]

[1]Department of Microbiology and Cell Biology, Indian Institute of Science, Bangalore, India

^ Current Address: Department of Molecular and Cell Biology, University of California, Berkeley, USA

[2]Centre of Infectious Disease Research, Indian Institute of Science, Bangalore, India

[3]Department of Biochemistry, Indian Institute of Science, Bangalore, India

[4]Department of Developmental Biology and Genetics, Indian Institute of Science, Bangalore, India

[5]Adjunct Faculty, School of Biology, Indian Institute of Science Education and Research, Thiruvananthapuram

*Corresponding author: Prof. Dipshikha Chakravortty

#Equal Contribution

Email: dipa@iisc.ac.in

Tel. No. 0091 80 22932842

Abstract

Foodborne pathogens pose a major global health hazard, worsened by drug-resistant strains. Therefore, designing novel therapeutic strategies is crucial. Here, we identified the protective role of gut-commensal *Odoribacter splanchnicus* (OS) against *Salmonella* in mice by promoting colonization resistance, preserving gut barrier integrity, and preventing acute inflammation and biofilm formation. *In vitro,* both OS and their culture supernatant inhibited *Salmonella* biofilm formation, intracellular proliferation in human intestinal cells, and

virulence gene expression. Further, our results depicted that OS's protective role acts over a broad spectrum as it confers protection against Gram-positive, *Listeria monocytogenes* and Gram-negative, *Salmonella* Typhimurium. Notably, OS conferred protection even when administered post-infection in mice, highlighting its therapeutic potential. Using several biochemical and proteomics approaches, we characterized key OS-secreted molecules that limit intracellular *Salmonella* and *Listeria* replication in human intestinal epithelial cells by regulating key virulence effectors and flagella. Collectively, our study establishes OS as the broad-spectrum protective agent against *Salmonella* and *Listeria* infections, with promising therapeutic potential.

Keywords: *Salmonella* pathogenesis, **Gut vascular barrier permeability**, **inflammation**, **inter-species bacterial regulation**, ***Listeria***, ***Odoribacter splanchnicus***, **gut commensal**, **biofilm, flagella**

Author Summary

Foodborne pathogens such as *Salmonella* and *Listeria* continue to threaten global health, especially with the rise of antibiotic resistance. In this study, we identify the gut commensal bacterium *Odoribacter splanchnicus* (OS) as a potent protectant against these pathogens. Using a mouse model, we show that OS enhances colonization resistance, maintains gut barrier integrity, and prevents both inflammation and biofilm formation during infection. Remarkably, OS also limits pathogen proliferation and virulence gene expression in human intestinal cells. These protective effects are mediated by both live OS and its secreted molecules within culture supernatant**.** Importantly, OS administration post-infection also conferred protection, indicating strong therapeutic potential. Biochemical and proteomic analyses revealed OS-secreted factors that suppress key virulence and motility pathways in pathogens. Our findings establish *Odoribacter splanchnicus* as a promising broad-spectrum biotherapeutic agent against major foodborne infections.

54

55

56 **INTRODUCTION**

57 The existence of the gut vascular barrier (GVB) acts as a protective barrier against the entry of
58 microorganisms into systemic blood circulation (1, 2). Enteric pathogens such as *Salmonella*
59 *enterica* can cross the mucus and intestinal epithelial barrier, ultimately leading to GVB
60 damage and systemic dissemination (1). The gut microbiota aids in the maintenance of the
61 intestinal epithelial barrier by the production of several metabolites such as short-chain fatty
62 acids (SCFAs), indoles, and polyphenol metabolites that contribute to epithelial barrier
63 integrity and turnover by regulating the expression of tight-junction (TJ) genes (3).
64 Additionally, these SCFAs have the potential to exert anti-inflammatory properties by
65 regulating cytokine production, mucosal immune cell migration, and secretion of antimicrobial
66 peptides (AMPs) by intestinal epithelial cells and macrophages (4-6).

67 *Salmonella* enters the body through the ingestion of contaminated food and water, resisting the
68 acidic stomach pH with acid tolerance response (ATR) genes, and finally reaches the lumen of
69 the small intestine(7). The pathogen gains entry into the non-phagocytic epithelial cells via
70 *Salmonella* Pathogenicity Island-1 (SPI-1) effectors to breach the intestinal barrier (8). Once
71 traversing through the mucosal lining of the gut epithelium, it reaches the lamina propria (8).
72 In the lamina propria, *Salmonella* encounters various host immune cells like neutrophils,
73 macrophages, and dendritic cells. Macrophages, dendritic cells, and neutrophils are responsible
74 for successful dissemination throughout the body through the reticulo-endothelial system
75 (RES) to the secondary organs such as Mesenteric Lymph Node (MLN), liver, and spleen(8).
76 *Salmonella* relies on the SPI-2 secretion for its intracellular and intravacuolar life by injecting
77 various virulence factors into the host cell cytosol (9, 10).

78 *Odoribacter splanchnicus* (OS, belonging to the order Bacteroidales, is a common member of
79 the human intestinal microbiota. *Bacteroidetes* is one of the major commensal phyla
80 dominating the healthy mouse as well as the human gut (11). It is a Gram-negative, anaerobic,
81 non-motile and non-spore-forming bacterium. A decrease in *Odoribacter* abundance has been
82 linked to different microbiota-associated diseases, such as non-alcoholic fatty liver disease,
83 cystic fibrosis, and inflammatory bowel disease (IBD)(12). A recent report indicated the ability
84 of OS and its effectors transported in Outer membrane vesicles (OMVs) to exhibit anti-
85 inflammatory effects on the gut epithelium(12). Further, OS has been implicated in conferring
86 resistance against colitis and colorectal cancer(13). This led us to hypothesize that *O.*
87 *splanchnicus* might ameliorate the inflammatory disease conditions associated with *Salmonella*
88 infection and dissemination. Here, in the present study, we aim to understand whether
89 colonization with the gut commensal OS, could ameliorate *Salmonella*-induced inflammation
90 and pathogenic dissemination.

91 Our study shows that OS colonization promotes colonization resistance of *Salmonella*, and
92 ameliorates systemic dissemination. OS ameliorates acute *Salmonella*-induced inflammation
93 and its associated pathogenesis by promoting colonization resistance, resulting in decreased
94 *Salmonella* invasion of gut tissue, the preservation of tight junctions, and GVB maintenance.
95 Further, we demonstrate that not only live OS but its culture supernatant inhibits *Salmonella in*
96 *vitro* biofilm formation, intracellular proliferation in human intestinal epithelial cells, and
97 virulence gene expression. Subsequently, our results depict that the specific protective role of
98 OS acts over a broad spectrum as it confers protection against both flagellated Gram-positive,
99 *Listeria monocytogenes* and Gram-negative, *Salmonella* Typhimurium. Furthermore, OS
100 conferred protection even after its administration to mice post-establishment of infection
101 highlighting its therapeutic potential. Subsequently, we identified the key OS-secreted
102 bacteriocin protein responsible for limiting intracellular *Salmonella* and *Listeria* replication in

103 human intestinal cells by regulating virulence genes such as flagella. Overall, our study
104 implicates the broad-spectrum protective role of OS in mitigating foodborne infections caused
105 by *Salmonella* and *Listeria* pathogenesis.

106 MATERIALS AND METHODS

107 Bacterial Strains and Culture Conditions

108 *Salmonella enterica* serovar Typhimurium (STM) strain ATCC 14028S, STM ATCC 14028S
109 constitutively expressing mCherry (pFPV25.1-mCherry-Amp^R, RFP), *Salmonella enterica*
110 serovar Typhi CT18 (STY), laboratory stock of *Enterococcus faecalis* strain API 142 MTCC
111 439 (ATCC 35550) (Ef), *Listeria monocytogenes* MTCC 657 (LM) expressing mCherry
112 (pFPV25.1-mCherry-Amp^R), and *Odoribacter splanchnicus* (OS) strain NCTC 10825
113 [1651/6] from ATCC were used in this study. 4% paraformaldehyde-fixed-OS was used as
114 killed bacteria control. The STM, LM, and Ef bacterial strain was grown overnight in Miller
115 LB broth (Himedia, M1245) at 37 ^{0}C under 160 rpm shaking conditions. OS was cultured under
116 anaerobic conditions (anaerobic chamber) in tryptic soy broth (Himedia, M-011) at 37ºC for
117 48-72h after its revival from glycerol stock.

118 Preparation of Cell-free Bacterial Culture Supernatant

119 The overnight grown OS culture in tryptic soy broth was centrifuged at 10,000rpm for 10 min
120 and the supernatant was harvested. The collected supernatant was further subjected to another
121 two rounds to centrifugation to remove any residual cells. The supernatant was subsequently
122 filtered using a 0.2 µm filter (Cole-Parmer PTFE Syringe Filters) and stored at − 20˚C.

123 Animal Experiments

124 The animal experiments were conducted in accordance with the approved guidelines of the
125 institutional animal ethics committee at the Indian Institute of Science, Bangalore, India

126 (Registration No: 48/GO/ReRcBiBt-S/Re-L/99/CPCSEA). All procedures involving the use of
127 animals were performed according to the Institutional Animal Ethics Committee (IAEC)-
128 approved protocol (CAF/Ethics/853/2021). 6–8 weeks old adult C57BL/6 male mice were used
129 in this study (bred, housed, and provided (purchased) by Central Animal Facility, Indian
130 Institute of Science, Bangalore). Male mice were used to minimize variability associated with
131 estrous cycle–dependent hormonal fluctuations that can modulate innate and adaptive immune
132 responses and influence infection outcomes. Using a single sex reduced experimental
133 variability and improved statistical power to detect infection-induced phenotypes within the
134 scope of this study. After one day of OS colonization (10^5 CFU/mice via oral gavage), the mice
135 were infected with 10^6 (organ burden) CFU or 10^8 CFU (for assessing survival) of *S.*
136 Typhimurium, and 10^8 (organ burden) or 10^9 (survival) CFU of *L. monocytogenes* via oral
137 gavage. The colonization of *O. splanchnicus* was confirmed via RT-qPCR mediated
138 quantitation of OS 16S rRNA from the mice fecal (3 fecal pellets harvested from the intestine
139 and resuspended in Trizol) and ileal samples at 6th day post-OS colonization. For post-infection
140 OS administration studies, OS was orally administered (10^5 CFU/ mice) post 1 or 3dpi. 5-day
141 post-infection, mice were euthanized, dissected out, and blood and organs were harvested. The
142 organs were homogenized using a bead-beater. The bacterial organ load was enumerated by
143 plating the tissue homogenates on *Salmonella-Shigella* (SS) agar plates for *Salmonella* or LB
144 plates containing 50µg/ml of Ampicillin for LM. The harvested tissues and the fecal samples
145 were collected in protein lysis buffer (RIPA) and TRIzol (Takara) for protein and RNA
146 extraction respectively and were stored at -80ºC. For calculating percentage survival, the
147 infected mice cohorts were monitored till fatality and fatalities were reported.

148 **Blood collection and serum preparation**

149 Blood collection was performed on the 5th day post-infection via cardiac puncture post-
150 euthanization of the mouse. The collected blood was allowed to clot by incubating the vials at

151 room temperature for 45 minutes. After allowing the standing time of 45 mins, centrifugation
152 was performed at 2000g for 15 minutes in a refrigerated centrifuge. Following the
153 centrifugation, the clear, yellowish supernatant was transferred to an autoclaved microfuge tube
154 and stored at -80ºC till further downstream processing.

155 **ELISA**

156 Cytokines in mice serum were quantified according to the manufacturer's instructions(10, 14).
157 Briefly, 96-well ELISA plates of IL-6 ELISA kit (BD Bioscience- Cat No-555240) were coated
158 overnight with capture antibody at 4°C. Following day, plates were washed with 0.1% Tween-
159 20 containing PBS and blocked with 10% FBS for 1 h. Following blocking, wells were washed
160 and incubated with 50µl of serum samples in duplicates for 2 h at room temperature.
161 Subsequently, plates were washed and incubated with detection antibody and enzyme reagent
162 for 1 h at room temperature (BD Bioscience). TMB (Sigma) was used as a substrate and
163 reactions were stopped with 2 N H_2SO_4.

164 Absorbance was measured at 450 nm wavelength in Tecan Plate reader and the concentration
165 of cytokines were interpolated from a standard curve.

166 **Quantitative Real Time PCR**

167 Total RNA was isolated from the ileal section of the intestinal tissues or feces harvested in
168 TRIzol (Takara) as per manufacturer's protocol. RNA was quantified using Nano Drop
169 (Thermo-Fischer scientific).3 µg of total isolated RNA was subjected to DNaseI (Thermo
170 Fischer Scientific) treatment at 37°C for 1 hr followed by heat inactivation at 75°C in the
171 presence of 5mM concentration of EDTA for 10 mins. The mRNA was reverse transcribed to
172 cDNA using oligo $(dT)_{18}$ primer, random hexamer primer, buffer, dNTPs and reverse
173 transcriptase (Takara) as per manufacturer's protocol. The expression profile of target gene was
174 evaluated using specific primers (Table-S2) by using SYBR green RT-PCR master mix

175 (Takara) in Applied Biosystems (Quantstudio 5) or BioRad Real time PCR instrument. β-actin
176 was used as an internal control for mammalian genes and for bacterial genes 16S rRNA was
177 used. All the reaction was setup in 384 well plate with three replicates for each sample.

178 **Western blotting**
179
180 The harvested tissue samples were lysed in ice-cold RIPA buffer (50 mM Tris-Cl, pH 8.0, 150
181 mM NaCl, 5mM EDTA, 1% NP-40, 1 % Sodium deoyxycholate, 1% SDS) containing protease
182 inhibitor cocktail (Roche). Total protein was estimated using Bradford reagent (BioRad).
183 Protein samples were denatured in **Laemmli SDS loading buffer** at 95ºC for 10 min and then
184 subjected to separation on 12% SDS-PAGE gels followed by transfer onto activated 0.45µm
185 PVDF membrane. Finally, the membrane was blocked with 5% skimmed milk in TBST (Tris
186 Buffered Saline containing 0.1% Tween-20) and probed with appropriate primary (Table-S3)
187 and secondary HRP-conjugated antibodies. The blots were developed using ECL substrate
188 (Bio-Rad) using a Chemidoc (BioRad). All densitometric analysis was performed using
189 ImageJ software.

190 **Immunohistochemistry**

191 The harvested tissues were fixed in 4% paraformaldehyde, embedded in paraffin and 5 µm
192 thick paraffin sections were collected on poly-lysine coated glass slides. The sectioned tissue
193 samples were deparaffinized using standard protocol. Briefly, the slides containing the
194 paraffinized tissues were immersed in xylene for 10 minutes and this step was repeated twice.
195 After the xylene treatment, the tissues were subjected to absolute alcohol treatment for 5
196 minutes twice, followed by 95% and 70% alcohol treatment for 5 minutes. The slides were
197 rinsed in water followed by boiling step in water for 2 minutes and then dried. For in vivo
198 estimation of biofilm, deparaffinized tissue samples were stained with Calcofluor White

199 (Sigma) stain for 20 min at RT. All immunofluorescence images were obtained using Zeiss
200 multi-photon 880 microscope and were analyzed using ZEN black 2012 software.

201 **Haematoxylin and Eosin Staining**

202 The harvested ileal tissues were collected and fixed using 3.5% paraformaldehyde. The fixed
203 liver was then dehydrated using a gradually increasing concentration of ethanol and embedded
204 in paraffin. 5µm sections were collected on coated plates. Sections were further rehydrated and
205 then stained with hematoxylin and eosin. Images were collected in a Leica microscope.

206 The scoring of the pathological changes is graded as 0-4; for each of the pathological lesions
207 (Severe/ marked -4; Moderate -3; Mild -2; Minor/minimum -1; No pathology -0) considering
208 the intestinal inflammation and associated villi injury as described previously (15, 16).

209 **Cell Culture**

210 Human colorectal adenocarcinoma cell line Caco-2 were maintained in Dulbecco's Modified
211 Eagle's Media (DMEM) (Lonza) and supplemented with 10% FCS (Fetal calf serum, Gibco)
212 and 1% non-essential amino acid solution (Sigma Aldrich) at 37ºC temperature in the presence
213 of 5% CO_2 in humidified incubator. Prior to each experiment, cells were seeded into 24 well
214 or 6 well plate as per requirement at a confluency of 60%.

215 **Intracellular proliferation or gentamicin protection assay**

216 Caco-2 epithelial were infected with 3 to 4 h old log phase STM or LM or STY bacterial culture,
217 STM (or LM or STY) with OS, STM (or LM or STY) in presence of *O. splanchnicus*
218 supernatant and STM along with PFA-fixed OS at an MOI of 10. For attachment of bacteria to
219 the cells, tissue culture plates were subjected to centrifugation at 600xg for 5 min and incubated
220 at 37 ^{0}C humified incubator with 5% CO_2 for 25 min. Following infection of the cells with
221 STM at an MOI of 10, cells were treated with DMEM (Sigma) + 10% FBS (Gibco) containing

222 100 µg/ml gentamicin for 1 hr. Subsequently, the gentamicin concentration was reduced to 25
223 µg/ml and maintained until the specified time point. Post 2hr and 16hr post-infection, cells
224 were lysed in 0.1% triton-X-100. Lysed cells were serially diluted and plated on *Salmonella-*
225 *Shigella* (SS) or LB agar to obtain colony-forming units (CFU). Percent invasion was
226 determined using the following formula (17, 18):

227 **Percent invasion= [CFU at 2 h]/ [CFU of pre-inoculum] X 100**

228 Fold proliferation was calculated as CFU at 16hr divided by CFU at 2hr.

229 **Fold Proliferation= [CFU at 16h] / [CFU at 2h]**

230 **Immunofluorescence confocal microscopic studies**

231 At the specified time points post infection with mCherry-tagged STMAS, cells were fixed with
232 3.5% paraformaldehyde for 15 min. Primary antibody staining was performed with specific
233 primary antibody in the presence of a permeabilizing agent, 0.01% saponin (Sigma) dissolved
234 in 2.5% BSA containing PBS at 4°C for overnight or for 6hr at room temperature (RT).
235 Following this, cells were washed with PBS stained with appropriate secondary antibody
236 tagged with fluorochrome for 1 hr at RT. This was followed by DAPI staining and mounting of
237 the coverslip onto a clean glass slide using the mounting media containing the anti-fade agent.
238 The coverslip sides were sealed with a transparent nail paint. All immunofluorescence images
239 were obtained using Zeiss Multiphoton 880 and were analyzed using ZEN Black 2012 software.

240 **Growth Curve analysis**

241 For *in vitro* growth curve experiments a single colony of STM and OS was inoculated in 5mL
242 of LB broth singly or in co-culture and grown overnight at 37ºC in anaerobic jar. In another
243 set, STM was inoculated in 5mL of LB in presence of OS supernatant. Overnight-grown
244 stationary phase bacteria were sub-cultured at a ratio of 1: 100 in freshly prepared LB in

245 presence or absence of OS supernatant and kept at 37ºC. At different time intervals, aliquots
246 were taken for measurement of [OD]600nm by TECAN 96 well microplate reader and were
247 plated for CFU enumeration.

248 **Biofilm-inducing growth media and conditions**

249 LB medium lacking NaCl and containing 1% casein enzyme hydrolysate (Hi-Media, India) and
250 0.5% yeast extract (Hi-Media, India)) was used as biofilm media as per previous literature (19).
251 Overnight grown culture was subcultured in 2 ml biofilm medium at the dilution of 1:100 in a
252 flat-bottom 24-well plate (Tarsons, India) and incubated at 28˚C for 72 h without shaking.

253 **Biofilm inoculation with OS culture supernatant**

254 20 µl of STM overnight culture and indicated volume (1% v/v or as indicated) of the OS culture
255 supernatants were added to 2 ml of biofilm media and incubated under biofilm-promoting
256 conditions(19). For co-culture experiments, the overnight cultures of the STM and OS or STM
257 and PFA-fixed OS were added in a 1:1 ratio to 2 ml of biofilm media and incubated under
258 biofilm-inducing conditions.

259 **Crystal Violet Staining**

260 Post 72 h of biofilm induction, the media was discarded, and the plates were thoroughly washed
261 in water. The plates were dried, and 2 ml of 1% Crystal Violet (CV) was added to each well
262 and incubated for 15 min. Post 15 min incubation, the CV stain was removed, and the plate was
263 thoroughly rinsed in water to remove excess stain. The stained biofilm was destained with 70%
264 ethanol, and the intensity of the colour of the destained solution was quantified at OD_{595} in the
265 Tecan plate reader (Infinite Pro 200) (19).

266 **Glass bead assay**

267 1 mm glass beads were added onto the pellicle to assess the strength of the pellicle at the air-
268 liquid interface. The initial weight of the glass beads was noted. The glass beads were added
269 until the pellicle collapsed, and the final weight was noted down and plotted.

270 **Gut Permeability Assay**

271 The infected mice cohorts were orally administered with FITC Dextran (25mg/kg of mice body
272 weight, FD-4-100MG, Sigma) 4h before euthanization. The blood plasma was collected post-
273 euthanization by cardiac puncture followed by centrifugation. The blood plasma was evaluated
274 for mean fluorescence via plate reader (TECAN) and flow cytometry(CytoFlex, Beckman).

275 **MTT Assay**

276 Post-16h treatment of pre-seeded Caco-2 cells with 10µg/ml of bacteriocin, MTT (3-(4,5-
277 dimethylthiazol-2-yl)-2,5-diphenyltetrazolium bromide) staining solution (0.5mg/ml) was
278 added to each well followed by incubation at 37ºC CO_2incubator for 4h. 50µl of DMSO was
279 added per well for solubilizing the formazan crystals. Absorbance was measured at 570nm
280 using a plate reader (TECAN).

281 **Transmission electron microscopy**

282 Overnight STM or LM-grown cultures (in the presence or absence of OS supernatant or
283 bacteriocin) were subcultured into fresh media (1:10) ratio and incubated at 37ºC for 6 hours
284 under shaking conditions. These samples were centrifugated at 1000rpm for 10 min to obtain
285 the bacterial pellet. The bacterial pellet was subjected to PBS wash twice via centrifugation at
286 1000 rpm for 10 min.5 µl of the finally resuspended cell suspension was added on a glow-
287 discharged copper-grid, air dried, stained with 1% uranyl acetate for 30 s, and visualized under
288 a transmission electron microscope (JEM-100 CX II; JEOL).

289 **Supernatant Treatment**

290 The supernatant was treated with 7.5 mM concentrations of EDTA and incubated at 65 °C for
291 1 h. 10 µl of proteinase-K (NEB, stock 20 mg/ml) was added to the 200 µl supernatant and
292 incubated at 37 °C for 1 h. The proteinase was inactivated with 0.5 mM PMSF and incubated
293 at 28 °C for 1 h. The supernatant was subjected to heating at 37˚C (60 min), 65˚C (15 min) or
294 95˚C (15 min) and immediately frozen at − 20˚C (19). Post-treatment, the supernatants were
295 used to inoculate the biofilm to test the nature of the biofilm inhibitory molecules.

296 **Supernatant concentration and molecular weight-based separation**

297 4 ml of the supernatants were transferred to the 3k MWCO or 10k MWCO Amicon ultra filter
298 centrifugal device (Amicon® Ultra-4 centrifugal filter device, 3k MWCO, UFC800324;
299 Amicon® Ultra-4 Centrifugal filter Unit, 10k MWCO, UFC801024) and centrifuged at 4000 g
300 for 30 min in a swing bucket rotor(19). The concentrated solute from the bottom of the filter
301 device and the flowthrough were collected and subjected to biofilm inoculation.

302 **Size Exclusion Chromatography**

303 The bacterial supernatant was concentrated to 0.5ml using 3k MWCO-Amicon-Ultra-4-
304 centrifugal unit and loaded onto the Superdex 200pg size exclusion column (XK16/60, 124mL;
305 Cytiva, USA), pre-equilibrated Tris-Cl buffer (pH-8) containing 100mM NaCl and 20mM Tris-
306 Cl. The sample was eluted with the same buffer at a flow rate of 0.8mL/min, and 1mL fractions
307 were collected. The fractions corresponding to the elution peaks were analyzed for biofilm
308 inhibition activity and subjected to mass spectrometry.

309 **LC/MS analysis of the supernatant fractions**

310 The concentrated gel filtration fractions of supernatants were subjected to in-solution trypsin
311 digestion for LC Q-TOF MS analysis. Briefly, 100 µg of total protein was resuspended in
312 100 µl of 7-8M of urea buffer. To this, 5 µl 200mM DTT was added and incubated at room
313 temperature for 1 hr, followed by alkylation with 20µl of 200 mM iodoacetamide and
314 incubation at room temperature for 1h in the dark. This was followed by the addition of 1mM
315 of Calcium chloride and incubation at RT for 10 min. For protein digestion, trypsin solution
316 was added to the sample to a final trypsin to protein ratio of 1:30 (w/w) and incubated at 37˚C
317 for 16 h, with frequent shaking. The reaction was stopped by adding 0.1% formic acid to adjust
318 the pH to 3-4. The digested protein samples were desalted using a reverse phase C-18 column
319 (Acclaim prep EASY-Spray (C18-RP)) using mobile phase solvent A-2% acetonitrile and
320 solvent B- 80% acetonitrile. The sample injection volume was 10µl. All the samples were
321 analyzed using Thermo Scientific SII for Xcalibur method. The MS scan was acquired using
322 Orbitrap detector with 60000 resolution in the positive polarity and scan range (*m/z*) 350-2000.
323 The ion source type was NSI with static voltage; positive ion (V)- 2200V and negative ion (V)-
324 600 along with temperature settings at 275ºC. This was followed by $ddMS^2$ IT HCD with 30%
325 fragmentation HCD collision energy using ion trap detector. The raw data was analyzed using
326 Proteome Discoverer 2.5 against the *O. splanchnicus* proteome available in UniProt (Proteome
327 ID: UP000006657).

328 **Purification of bacteriocin**

329 *O. splanchnicus* culture supernatant was concentrated within the range of >3kDa and <10kDa
330 using the Amicon Ultra-4 Centrifugal filter units of 10MWCO and 3MWCO. The concentrated
331 cell-free supernatant containing the bacteriocin (~7kDa) was precipitated by ammonium
332 sulphate (80% to 98%). The precipitate was collected by centrifugation at 12000rpm for 30
333 min and dissolved in 1X PBS. The dissolved precipitate was again filtrated using the 3KDa

334 cutoff Amicon centrifugal filter units. This concentrated fraction was further subjected to Fast
335 Performance Liquid Chromatography using Superdex 75 Increase 10/300 GL- 24ml volume
336 (GE Healthcare) column. The column was equilibrated with 1X Phosphate Buffered Saline
337 buffer and 0.5ml of concentrated sample (23.6 mg/ml) was injected into the column. Based on
338 the increase in Absorbance units at 280nm from baseline, 0.3ml fractions were collected at a
339 retention volume of 13.3ml to 21.8ml (Fig. S8). The fractions were analyzed by 20% SDS-
340 PAGE electrophoresis and stained with Coomassie staining solution.

341 ***In vitro* swim motility assay**

342 2 µl ($2*10^6$ CFU/ml) of treated or untreated stationary phase bacterial samples were spotted on
343 the 0.3% agar (LB-STM, BHI-LM) plates supplemented with 0.5% yeast extract, 1% casein
344 enzyme hydrolysate, 0.5% NaCl, and 0.5% glucose. The plates were incubated at 37˚C and
345 images were taken every 6 h (STM) or 24h (LM) using the camera of Biorad illuminator.

346 **Statistical analysis**

347 Data were analyzed and graphed using the GraphPad Prism 8 software (San Diego, CA).
348 Statistical significance was determined by Student's t-test or One-way ANOVA followed by
349 Dunnett's Multiple Comparisons test to obtain p values. ANOVA was used during comparison
350 among three or more groups whereas Student's t-test was used to compare the difference
351 between two groups. Mann Whitney t-test was used as a non-parametric counterpart of Student
352 t-test when variances differed. The log-rank test also known as Mantel-Cox test is used to
353 compare the survival percentages of the mice groups. Adjusted p-values below 0.05 are
354 considered statistically significant (****$p<0.0001$, *** $p < 0.001$, ** $p<0.01$, * $p<0.05$). The
355 results are expressed as mean ± SD or SEM of three independent experiments.

356

357 **RESULTS**

358 ***O. splanchnicus* hinders *Salmonella* burden and its systemic dissemination**

359 To denote the role of OS in *Salmonella* pathogenesis, we colonized C57BL/6 mice with 10^5
360 CFU of OS 1 day prior to *Salmonella* infection via the oral route and validated the colonization
361 by undertaking OS 16S rRNA qPCR analysis (Fig 1, A-B). OS pre-colonized mice showed
362 decreased susceptibility to *Salmonella* infection in comparison to the non-colonized mice
363 cohort which succumbed to death by day 9 post-infection (p.i.). Contrastingly, 100% of the OS
364 colonized mice were alive even at day 11 post *Salmonella* infection (Fig 1, C). *Salmonella*
365 colonization of the feces and intestinal tissue and dissemination to the MLN, blood, and liver
366 were reduced upon OS pre-colonization (Fig 1, D-K). OS non-colonized mice exhibited
367 increased weight loss percentage upon *Salmonella* infection and OS pre-colonization prevented
368 weight loss (Fig 1, H). Our result suggests OS could ameliorate *Salmonella* colonization, organ
369 burden and dissemination (Fig 1).

370 ***O. splanchnicus* colonization ameliorate the acute *Salmonella-induced* inflammation and**
371 **its associated pathogenesis**

372 Heightened inflammatory responses facilitate *Salmonella* dissemination in mice(20). Thus, we
373 hypothesized that OS gut colonization might ameliorate the *Salmonella*-induced inflammation.
374 ELISA-mediated IL-6 serum quantification revealed reduced IL-6 production upon *S.*
375 Typhimurium (STM) infection in the OS colonized mice group to the non-colonized cohort
376 (Fig 2, A). To combat the enteric pathogen challenge, the host employs one of its major defence
377 arsenals, that is, the production of antimicrobial peptides (AMPs)(21, 22). STM infection
378 induces enhanced mRNA expression of AMPs in mice with respect to the uninfected control
379 as per previous literature findings (17). We found that OS colonization in mice prevented STM
380 infection-induced expression of several AMP genes such as Lysozyme-C1 precursor,

381 Angiogenin-4 precursor, CCL20, and Regenerating-islet-derived 3 beta-precursor (Fig 2, B).
382 The haematoxylin eosin-stained intestinal sections suggested increased intestinal tissue
383 damage with irregularly organized villi, necrotic submucosa layer, neutrophil infiltration, and
384 detached intestinal cells in all the STM-infected non-OS-colonized cohorts. However, OS pre-
385 colonization restored the intestinal tissue architecture in all the mice cohorts (Fig 2, C-D).

386 ***O. splanchnicus* restricts *Salmonella*-mediated GVB damage and promotes tight junction**
387 **gene expression**

388 *Salmonella* breaches the gut vascular barrier (GVB) by inducing tight junction disruption.
389 *Salmonella* like other food-borne antigens enters into the Mesenteric Lymph Node (MLN) by
390 accessing the lymphatics and subsequently gains entry into the liver via the bloodstream(23).
391 The translocation of the pathogen across the blood endothelial cells is governed by the integrity
392 of the GVB(1). The GVB refers to the endothelial barrier and the microvasculature
393 characterized by the elaborate framework of the junctional complexes (1). The GVB
394 architecture is maintained by several tight junctions and adherens junction proteins that control
395 paracellular trafficking(24, 25). Other cell types associated with the microvasculature of the
396 GVB forming a vascular unit includes pericytes and fibroblasts(26). PV-1 (plasmalemma-
397 vesicle associated protein-1) expression is a marker of GVB damage and heightened PV-1
398 expression denotes EC permeability(27, 28). Our data show reduced *PV-1* marker expression,
399 alongside enhanced tight junction protein mRNA expression, such as *Tjp1* and *Claudin5*, upon
400 OS colonization during *Salmonella* infection in comparison to the non-OS-colonized cohorts.
401 (Fig. 3, A). Previous studies in *Mycobacterium marinum* have shown that transcriptional
402 induction of pro-angiogenic markers like *Vegfa* contributes to increased bacterial burden and
403 dissemination(29). In our study, OS pre-colonization in the gut resulted in reduced expression
404 of the pro-angiogenic *Vegfa* in the infected liver tissues, which coincided with the reduced *S.*
405 Typhimurium burden in the bloodstream and liver (Fig S1, A). Previous literature suggested

406 reduced expression of *Axin2,* a β catenin target gene, upon wildtype *Salmonella* infection, even
407 after Wnt3a stimulation suggesting that *Salmonella* affects the GVB by inhibiting canonical
408 Wnt signalling (1). Here, our results suggest that OS pre-colonization restores the *Salmonella*-
409 triggered attenuated Wnt signalling response with increased Axin2 expression in the
410 *Salmonella*-infected intestinal tissues (Fig. S1, B). The integrity of the infected mice gut was
411 estimated by the gut permeability assay using FITC-Dextran (Fig. 3, B). Our results indicate
412 increased gut vascular permeability upon *Salmonella* challenge which declined upon OS pre-
413 colonisation, implicating the ability of OS to prevent gut barrier disruption.

414 ***O. splanchnicus* culture supernatant restricts *Salmonella* biofilm formation and**
415 **intracellular proliferation in human intestinal cells**

416 To delineate the mechanism behind the protective role of OS against *Salmonella* pathogenesis,
417 we performed *Salmonella* infection studies in human intestinal epithelial cell line Caco-2 in
418 the presence of OS. The intracellular survival assay suggested decreased STM invasion and
419 subsequently attenuated intracellular replication within the infected Caco-2 cells upon co-
420 infection with live OS and in the presence of OS culture supernatant (Fig 4, A-B). However,
421 STM co-infection with fixed OS showed percent invasion and intracellular replication like that
422 of STM infection (Fig 4, A-B). Together, these results hinted at the presence of some secreted
423 inhibitory components in the OS culture supernatant that has the propensity to limit STM
424 infection. The reduced invasion and proliferation of STM within Caco-2 cells in presence of
425 OS was subsequently validated in immunofluorescence studies, wherein STM showed a
426 significant reduction in invasion at 2hr p.i. and intracellular proliferation at 16hr p.i. in case of
427 OS co-infection (Fig 4, C-D). Similar results were obtained upon infection with the human-
428 restricted serovar STY to the Caco-2 cells wherein OS and its supernatant attenuated STY
429 invasion and intracellular replication (Fig. 4, E-F). Further, we assessed the *in vitro* growth of
430 the STM in co-culture conditions with OS or in the presence of OS culture supernatant in

431 anaerobic conditions to mimic the microaerophilic or hypoxic environment of the gut or in
432 aerobic culture conditions. We observed no significant delay *in vitro* growth of STM at its
433 initial lag to log phase of its growth in the presence of OS supernatant or with live OS under
434 anaerobic culture conditions (Fig S2, A-B). In aerobic growth conditions as well, *Salmonella*
435 growth remained unperturbed even in the presence of OS or its culture supernatant (Fig S2, C-
436 D). Several previous studies have corroborated the ability of commensal bacterial culture
437 supernatants to inhibit colonization and the biofilm formation of several pathogens. For
438 instance, a commensal bacterium, *Staphylococcus epidermis*, could inhibit biofilm formation
439 and nasal colonization of its pathogenic counterpart, *Staphylococcus aureus* (30). Moreover,
440 biofilm formation is also regulated at the interspecies level. Indole is an inter-species biofilm
441 regulator that decreases *E. coli* biofilm formation and facilitates biofilm formation of
442 pseudomonads (31). STM forms biofilm to colonize the host, evade host defence arsenals and
443 antibiotics, persist during chronic infections, and transmit to new hosts (32, 33). We, therefore,
444 examined the biofilm pellicle strength and biofilm formation of STM via crystal violet staining
445 on the solid-liquid interface in the presence or absence of live, PFA-fixed-OS or OS culture
446 supernatant by inoculating STM in biofilm-inducing media with low salinity. STM exhibited
447 biofilm formation defect in the presence of live OS or OS supernatant (Fig 4, G). However, the
448 STM biofilm inhibitory property of OS was diminished upon treatment with paraformaldehyde
449 (PFA)-fixed OS (Fig 4, G). Further, qPCR-mediated gene expression studies of *Salmonella*
450 biofilm genes revealed decreased expression of genes regulating biofilm (*csgD*, *csgA*, *bapA*)
451 under treatment with live OS or its culture supernatant (Fig.4, H-J). Flagella-mediated
452 attachment and several virulence factors such as SPI-1 and SPI-2 genes are responsible for
453 *Salmonella* pathogenesis and its biofilm formation (19, 34, 35). Therefore, we evaluated a few
454 of the *Salmonella* flagellar and SPI-1 and SPI-2 gene expression in the presence or absence of
455 OS or its culture supernatant via quantitative real-time PCR. Our results depicted attenuated

456 expression of flagellar gene (*fliC*), SPI-1 (*sipC*) and SPI-2 (*pipB2*) genes both in the presence
457 of live OS and its spent media but not in presence of PFA fixed-OS (Fig. 4, K-M). The loss in
458 *Salmonella* flagellar motility was further validated via TEM imaging wherein OS or its
459 supernatant reduced the flagella formation of *Salmonella* considerably (Fig.4, N). Together,
460 our results implicate the ability of OS to inhibit STM biofilm formation via active secretion of
461 certain inhibitory molecules in the supernatant.

462 ***O. splanchnicus* inhibitory effect on *Salmonella* is specific as *Enterococcus faecalis*,**
463 **another gut resident microbe, fail to inhibit *Salmonella* intracellular proliferation or**
464 **biofilm formation**

465 The resident gut microbes provide colonization resistance against invading pathogens by
466 deploying several mechanisms, including the production of inhibitory molecules, nutrient
467 competition, maintenance of the intestinal epithelial integrity, immune activation, and via the
468 deployment of bacteriophages (36, 37). To understand whether our observed inhibitory trait of
469 OS against *Salmonella* is due to a common colonization restriction phenomenon of gut
470 microbes via competitive inhibition, or it is a specific phenomenon, we evaluated the role of
471 another gut resident microbe, *Enterococcus faecalis* on *Salmonella* intracellular replication in
472 human intestinal epithelial cells and *Salmonella* biofilm formation. *Enterococcus sp.* belong to
473 the phylum of Firmicutes in the family Enterococcaceae. Approximately, 10^6-10^7 *Enterococcus*
474 *sp*. reside in the human intestine with major abundance of *E. faecalis* (10^5-10^7 CFU/gm feces)
475 and *E. faecium* (10^4-10^5/gm feces) (38). *E. faecalis*, *E. faecium*, *Bifidobacterium sp*.
476 *Lactobacillus sp.,* and *E. coli* colonize the gut of healthy breastfed infants during the initial 7-
477 10 days post birth (39). Our intracellular survival assay data showed no defect in *Salmonella*
478 invasion or intracellular replication capability in Caco-2 cells in presence or absence of *E.*
479 *faecalis*, its culture supernatant or PFA-fixed *E. faecalis* (Fig. S3, A-B). Moreover, *E. faecalis*
480 or its *E. faecalis* supernatant did not inhibit *Salmonella* biofilm formation (Fig. S3, C).

481 Together, our results suggest the inability of *E. faecalis* to inhibit *Salmonella* invasion,
482 intracellular proliferation or its *in vitro* biofilm formation, thereby highlighting the specificity
483 of OS in restricting *Salmonella* pathogenesis.

484 ***O. splanchnicus* confers protection against another foodborne pathogen *Listeria***
485 ***monocytogenes***

486 To understand whether OS exerts a common broad-spectrum protection or colonization
487 resistance against other foodborne pathogens such as *Listeria monocytogenes*, we orally
488 infected 6-8-week-old C57Bl/6 mice with 10^8 CFU of *L. monocytogenes* (LM) 1 day post
489 colonization with 10^5 CFU of *O. splanchnicus* for organ burden evaluation via oral gavage. For
490 survival study, mice were orally gavaged with 10^9 CFU of *L. monocytogenes*. OS-colonized
491 mice exhibited increased survival rates upon LM challenge compared to the non-colonized
492 mice cohort (Fig. 5, A). In line with the survival data, the increased bacterial burden was
493 observed in the blood, feces, intestinal tissue, MLN, spleen and liver alongside enhanced
494 percent loss in mice body weight in the case of *Listeria* infection in non-colonized mice group
495 with respect to OS-precolonized- mice group (Fig. 5, B-J). In a similar line to *Salmonella*
496 infection, OS mitigated host antimicrobial response with reduced expression of antimicrobial
497 peptide transcripts during LM infection, amounting to reduced intestinal tissue damage.
498 Further, OS promoted tight junction functions during *Listeria* infection with reduced
499 expression of GVB damage marker, *PV-1* and angiogenesis marker, *Vegf* expression (Fig. S4,
500 A-C). Moreover, OS colonization could restrict the *in vivo Salmonella* and *Listeria* biofilm-
501 like microcolonies within the spleens of the infected mice cohorts as opposed to the non-
502 colonized mice cohorts (Fig.S4, D-E). We estimated the communities of bacterial cells within
503 the spleen tissue via Calcofluor white staining (40). Calcofluor white stains the biofilm matrix
504 or extracellular polymeric substances (EPS) comprised of cellulose (40, 41) and
505 exopolysaccharides that help in the adherence of the bacterial cells. This is the first study

506 demonstrating biofilm-like bacterial colonies of *Salmonella* or *Listeria* secreting EPS in
507 spleens. Like *Salmonella*, *in vitro* culture of *Listeria* with OS or its culture supernatant led to a
508 loss in flagella as evidenced via the TEM imaging (Fig.S4, F). Since flagella is one of the
509 factors facilitating biofilm formation and invasion, OS could inhibit both *Salmonella* and
510 *Listeria* colonisation and biofilm formation. Further, LM exhibited attenuated intracellular
511 proliferation within human intestinal Caco-2 cells upon live OS or OS supernatant treatment
512 (Fig. 6). Altogether, this result hints at the potency of OS to act broadly against Gram-positive
513 and Gram-negative bacteria.

514 **The protective role of *O. splanchnicus* against *Salmonella* Typhimurium and *Listeria***
515 ***monocytogenes* persists even on administration post-establishment of infection**

516 Next, we sought to examine whether the protective role of OS against *Salmonella* and *Listeria*
517 is sustained when the infection has been fully developed and whether it can serve as a treatment
518 regimen against foodborne diseases. Our results indicate the protective ability of OS against
519 both foodborne pathogens in their intestinal phase of infection when administered at 1-day
520 post-infection (dpi) as depicted by lower pathogen loads in all the organs and blood along with
521 reduced percent weight loss at 5th-day post-*Salmonella* or *Listeria* challenge in the OS-
522 administered (1-dpi) cohort when compared to the untreated cohorts (Fig. 7,A-K, Fig. S5, A-
523 C). Although the protective ability of OS persists even upon establishment of infection when
524 administered at 3rd-day post-*Salmonella* or *Listeria* challenge as indicated by reduced organ
525 loads and percent weight loss in the OS-colonized cohorts, the extent of protection is lower
526 compared to its administration at 1-dpi (Fig. 7, L-W, Fig. S5, D-S), Further, the OS challenge
527 at 1-dpi reduced the mice's susceptibility to the *Salmonella* and *Listeria* challenge(Fig. 7, L,R).
528 However, administration of OS at 3-dpi delayed the death of the *Salmonella* and *Listeria*-
529 infected mice cohorts by 1 day (Fig. 7, L,R). In line with the survival and organ burden data,
530 OS treatment at both 1st and 3rd dpi reduced both *Salmonella* and *Listeria*-induced GVB

531 damage with reduced PV-1 expression, AMPs, and *Vegf* expression, alongside promoting tight
532 junction protein (*Tjp1* and *Claudin5*) and *Axin2* expression (Fig. S5, D-M). However, OS
533 administration at 3-dpi conferred less protection than at 1-dpi as indicated by the protein
534 expression profiles of PV-1, and tight junction protein ZO-1 (Fig. S5, N-O). Additionally, OS
535 colonization mitigated gut vascular permeability during *Salmonella* and *Listeria* challenges as
536 indicated by reduced FITC-dextran fluorescence units in the plasma both upon pre or post-OS
537 colonization (Fig. S5, P). Moreover, the hematoxylin- eosin-stained intestinal sections revealed
538 reduced intestinal tissue damage with restoration in the villi architecture in the 1- and 3-dpi
539 OS-administered mice cohorts compared to the non-OS-treated groups (Fig.S5, Q).

540 Moreover, OS colonization could restrict the *in vivo Salmonella* and *Listeria* biofilm within the
541 spleens of the infected mice cohorts as opposed to the non-colonized mice cohorts both when
542 administered at 1-day and 3-day post-pathogen challenge. (Fig.S5, R-S).

543 **Characterization of the inhibitory active molecule within *O. splanchnicus* culture**
544 **supernatant**

545 Our results suggested that not only live OS but also its spent culture supernatant could inhibit
546 *Salmonella* invasion and intracellular proliferation in intestinal human epithelial cells.
547 Moreover, the OS and its supernatant could inhibit STM biofilm formation *in vitro.* This
548 inhibitory effect disappeared upon co-culture with paraformaldehyde-fixed-OS indicating the
549 presumable role of certain inhibitory microbial products secreted by metabolically live OS. To
550 delineate the nature of the secreted molecule/s, we subjected the supernatant to various
551 conditions such as high temperature, divalent cationic chelator, EDTA, and protease (proteinase
552 K), and subsequently assessed the biofilm formation (Fig. 8, A-C). Our biofilm assay suggested
553 that the active molecule is resistant to EDTA treatment and is stable at higher temperatures
554 (Fig. 8, A-B). Nevertheless, the active molecules within the fraction were sensitive to the

555 proteinase K treatment, suggesting the possibility of being protein in nature (Fig. 8, C). SDS-
556 PAGE of the OS supernatant revealed the size of the differential proteins with respect to the
557 media control ranged below 65kDa. (Fig. 8, D). Concentration-dependent estimation of the
558 biofilm activity of the supernatant revealed that the active molecules retain their activity at a
559 minimal concentration of 0.4% v/v (Fig. 8, E). We further fractionated the supernatant using
560 an Amicon 3k MWCO and 10k MWCO ultra filter device (Fig. 8, F-G). We found that the
561 active molecule/s is/ are higher than 3kDa cut-off range eliminating the role of small molecules
562 and ions (Fig. 8, F-G). A summary of the conditions tested for active molecule characterisation
563 and their effective outcome has been summarized in Fig. 8, H. Subsequently, we subjected the
564 culture supernatant to gel filtration chromatography (Fig. S6, A). Out of all the fractions tested,
565 around 24 fractions showed a biofilm inhibitory role. These 24 fractions were further subjected
566 to a titration experiment to zero down upon the three fractions with the highest inhibitory
567 activity (A82,A83,A84) (S6, B-D). The gel filtration standard curve run suggested that the
568 active molecules fall in the size range of <60kDa and >3kDa (Fig. S6, A). These three fractions
569 along with the total concentrated supernatant (serving as positive control) and fractions with
570 no or least inhibitory activity (serving as negative control-A31,B12) were ultimately subjected
571 to Reverse Phase LC-MS mass spectrometry. Upon analysis of the proteomics dataset (Fig. S6,
572 E), we obtained 364 proteins showing enrichment in the positive fractions. Among the 364
573 proteins, 74 proteins exhibited known or predicted function as per UniProt and STRING
574 database and 11 proteins were linked to antibacterial, bacteriostatic, flagella, and biofilm
575 regulation based on data curation and literature survey (Table-S1). We selected bacteriocin
576 proteins exhibiting direct association with antibacterial activity for further analysis. These
577 proteins include bacteriocins (A0A412WSU3 and A0A412WSS0) which are antimicrobial
578 peptides that can kill or inhibit closely related or unrelated bacterial strains(42, 43). We purified
579 the bacteriocins via ammonium sulphate precipitation followed by gel filtration

580 chromatography to obtain a single fraction comprising of bacteriocins with close-range
581 molecular weight (6.6 kDa and 7.156kDa, respectively) (Fig. S7).

582 ***O. splanchnicus*-derived purified peptide, bacteriocin, limits both *Salmonella* and *Listeria***
583 **pathogenesis *in vitro***

584 Treatment of the Caco-2 cells with the purified bacteriocin inhibited STM, STY, and LM
585 invasion and fold proliferation without compromising host-cell viability (Fig. 9, A-D).
586 Additionally, the purified bacteriocin treatment inhibited STM biofilm formation in a dose-
587 dependent manner alongside reduced transcript level expression of *Salmonella* biofilm
588 regulatory genes (Fig. S8, A-D). Moreover, bacteriocin treatment (10µg/ml) attenuated
589 *Salmonella* virulence gene expression such as SPI-1 gene- *sipC*, SPI-2 gene-*pipB2,* and
590 flagellar gene *fliC* (Fig. S8, E-G). Subsequently, TEM imaging revealed a complete loss of
591 *Listeria* flagella upon treatment with the OS-derived bacteriocin in contrast to *Salmonella*
592 which retained few flagella even on bacteriocin treatment (Fig. 9, E-H). Furthermore, the
593 motility assay demonstrated a significant swimming defect of *Listeria* and *Salmonella* upon
594 treatment with either OS supernatant or bacteriocin to the untreated control (Fig. 9, I-J).
595 Overall, our study depicts the novel role of OS-derived bacteriocin in limiting *Salmonella* and
596 *Listeria* invasion and pathogenesis by regulating virulence effectors such as SPI-1, SPI-2
597 genes, biofilm regulatory genes, and flagella.

598 **DISCUSSION**

599 *Salmonella* gains access to the systemic sites by traversing the gut intestinal barrier via utilizing
600 several routes. Its primary site of entry is the distal ileum wherein it induces the SPI-1 Type
601 Three Secretion System (T3SS) effector proteins to facilitate its uptake. After its initial entry
602 into the enterocytes and M-cells overlying the Peyer's patches, *Salmonella* colonizes the
603 draining MLN and eventually disseminates to the liver and spleen via the circulating

604 lymphatics and the bloodstream (44). *Salmonella* uptake by M cells facilitates its stealthy entry
605 via avoidance of the mucus barrier. Additionally, the presence of flagella allows them to propel
606 through the viscous mucus and activate the immune responses(45). The onset of systemic
607 dissemination coincides with GVB disruption and loss of tight-junction protein expression (1).
608 Several reports have suggested the protective role of gut commensals in maintaining gut
609 epithelial health against food-borne pathogen insults. *E. coli* provide colonization resistance
610 against STM in the presence of a specific microbial consortium by limiting galactitol wherein
611 *Lachnospiraceae* consume the free sugar, conferring colonization resistance (46). Moreover,
612 *E. coli* contribute to colonization resistance by competing with *S.* Enteritidis for aerobic
613 respiration (47). Similarly, the commensal *Klebsiella michiganensis* retention or transmission
614 provided colonization resistance to Enterobacteriaceae by exhibiting nutrient competition (48).

615 Previous literature hinted toward the beneficial effects of OS in healthy human gut wherein
616 reduced OS abundance have been linked to obese gut signature (49). Furthermore, OS
617 colonization in mice have been shown to enhance $Foxp3^{+}/ROR\gamma t^{+}$ regulatory T cells,
618 interleukin IL-10 and short chain fatty acids production, limiting colitis in mouse models (50).
619 OS have been depicted to confer protection against colitis and colorectal cancer in mice by
620 inducing intestinal Th17 development(13).

621 In this study, we report the broad-spectrum protective role of the gut commensal of
622 bacteroidales order *O. splanchnicus* that limits *Salmonella* and *Listeria* invasion, pathogenesis,
623 and systemic dissemination by promoting colonization resistance and regulating virulence
624 effectors such as SPI-1, SPI-2, flagella, and biofilm regulatory genes. Additionally, not only
625 OS but its culture supernatant could exert its inhibitory effect on *Salmonella* invasion and
626 intracellular proliferation in intestinal human epithelial cells. Moreover, the OS and its
627 supernatant could inhibit STM biofilm formation by regulating flagella formation. This STM
628 biofilm inhibitory effect was however lost upon co-culture with paraformaldehyde-fixed-OS

629 indicating the presumable role of certain inhibitory microbial products secreted by
630 metabolically live OS. Further, our studies identified OS-produced bacteriocins responsible for
631 restricting intracellular replication of *Salmonella* and *Listeria* in intestinal epithelial cells by
632 regulating bacterial virulence arsenals such as biofilm regulatory genes, SPI-1, SPI-2 genes,
633 and flagellar machinery. However, the presence of flagella on *Salmonella* post-bacteriocin
634 treatment suggests the potential involvement of additional secreted accessory molecules within
635 the OS supernatant and indicates that bacteriocins might act in concert with additional factors
636 through diverse mechanisms, warranting future research. Bacteriocin-mediated suppression of
637 several virulence-associated phenotypes with minimal impact on overall bacterial growth
638 suggests that the bacteriocin may interfere with regulatory pathways controlling virulence. One
639 possible mechanism is the modulation of global regulatory networks that coordinate virulence
640 gene expression, potentially through subtle physiological perturbations or cellular signalling
641 pathways. Such physiological changes could attenuate virulence programs including motility
642 required for host cell invasion and intracellular survival. Alternatively, bacteriocin exposure
643 may induce stress responses that indirectly downregulate energy-intensive virulence processes.
644 However, determining the precise molecular mechanisms underlying these effects will require
645 dedicated mechanistic studies, such as transcriptomic, proteomic, or regulatory pathway
646 analyses, which are beyond the scope of the present study but warrant further investigation in
647 future work.

648 Although the bacteriocin demonstrated significant anti-virulence activity in vitro, its
649 proteinaceous nature presents potential challenges for oral therapeutic applications due to
650 susceptibility to degradation in the gastrointestinal environment. Consequently, oral
651 administration experiments in mice were not pursued in this study. Future work should
652 therefore explore strategies to enhance stability and delivery, such as encapsulation and

653 protective formulations. Addressing these challenges will be important for translating
654 bacteriocin-based approaches into practical therapeutic applications.

655 Previous studies have suggested that bacteriocin expression by commensal bacteria can
656 influence gut niche competition and bacteriocin delivery can serve as an effective therapeutic
657 strategy to eliminate colonization of multi-drug resistant bacteria in the gastrointestinal tract
658 without disrupting the indigenous microbiota (51, 52). Several studies have highlighted the role
659 of commensal-produced bacteriocins. Bacteriocin-producing *Streptococcus salivarius* has been
660 shown to effectively target the CRC-causing pathogen *Fusobacterium nucleatum* in a model of
661 the human distal colon(53). *Lactobacillus plantarum* bacteriocin has been linked to intestinal
662 and systemic improvements in diet-induced obese mice and confers epithelial barrier integrity
663 (54). Further studies show that a class IIa bacteriocin, Pediocin PA-1, has an anti-bacterial
664 effect against *L. monocytogenes* (55).

665 Bacteriocins produced by commensal bacteria are typically characterized by strong bactericidal
666 activity that directly inhibits the growth of competing microorganisms. In contrast, the OS-
667 derived bacteriocin described in this study primarily suppressed virulence-associated
668 phenotypes including motility, SPI-1 and SPI-2 gene expression, and intracellular proliferation
669 without markedly impairing bacterial growth. This observation suggests that, rather than acting
670 solely as a classical antimicrobial compound, the OS-bacteriocin may interfere with regulatory
671 pathways controlling virulence. One possible mechanism is the modulation of global regulatory
672 networks that coordinate virulence gene expression, potentially through subtle physiological
673 perturbations or cellular signalling pathways. Alternatively, bacteriocin exposure may induce
674 stress responses that indirectly downregulate energy-intensive virulence processes. However,
675 determining the precise molecular mechanisms underlying these effects will require dedicated
676 mechanistic studies, such as transcriptomic, proteomic, or regulatory pathway analyses, which
677 are beyond the scope of the present study but warrant further investigation in the future. OS-

678 derived bacteriocin's virulence-modulating activity is conceptually distinct from many
679 previously described commensal-derived bacteriocins that mainly exert growth-inhibitory
680 effects. The ability to attenuate virulence while exerting limited pressure on bacterial viability
681 may represent a potentially advantageous strategy, as anti-virulence approaches are thought to
682 impose reduced selective pressure for resistance compared with conventional bactericidal
683 agents. Nevertheless, further mechanistic studies will be required to determine whether this
684 effect arises from direct interference with virulence regulatory networks or from broader
685 physiological perturbations induced by bacteriocin exposure.

686 This study provides evidence about inter-species regulation of gut colonization in maintaining
687 gut homeostasis and protecting against several invading foodborne pathogens. Moreover, the
688 long-term protective ability conferred by OS during pre-or post-infection colonization to mice
689 against broad-spectrum foodborne pathogens such as *Salmonella* and *Listeria* highlights its
690 therapeutic potential as a prebiotic for prophylaxis or post-infection treatment option, paving
691 the way for future therapeutic interventions to thwart food-borne infections.

692

693 **ACKNOWLEDGEMENTS**
694 We thank Nikhita Kirthivasan for her support during the commencement of the project.
695 We also thank our Divisional Mass Spectrometry facility, TEM facility, Departmental
696 Confocal Facility, Divisional Flowcytometry Facility and Central Animal Facility at IISc.
697 **FUNDING**
698 This work was supported by the DAE SRC fellowship (DAE00195) and DBT-IISc partnership
699 umbrella program for advanced research in biological sciences and Bioengineering to DC.
700 Infrastructure support from ICMR (Centre for Advanced Study in Molecular Medicine), DST
701 (FIST), UGC (special assistance) and TATA fellowship is highly acknowledged.
702 DH sincerely acknowledges the CSIR- SPM fellowship for her financial support.
703 DM and RV are supported by MHRD-GATE and CSIR fellowships respectively.
704 The funders had no role in study design, data collection and analysis, decision to publish, or
705 preparation of the manuscript.

AUTHOR CONTRIBUTION

Conceptualization: DH, DC

Methodology: DH, DM, RV, VD (Gel Filtration Chromatography), DD (Fast Performance Liquid Chromatography)

Investigation: DH, DM, RV, VD (Gel Filtration Chromatography), DD (Size exclusion chromatography for bacteriocin purification), RSR (Scoring of haemoxylin and eosin-stained samples)
Visualization: DH, DM, RV
Formal analysis: DH
Funding acquisition: DC
Project administration: DH, DC
Supervision: DC, UT (Proteomics), TH (Size Exclusion Chromatography),
MG (Size Exclusion Chromatography)
Writing – original draft: DH
Writing – review & editing: DH, DM, RV, RSR, VD, DD, TH, MG, UT, DC

COMPETING INTERESTS Authors declare that they have no competing interests.

DATA AND MATERIALS AVAILABILITY

All data are available in the main text or the supplementary materials.
The article has been submitted to the preprint server (56).

REFERENCES

1. Spadoni I, Zagato E, Bertocchi A, Paolinelli R, Hot E, Di Sabatino A, et al. A gut-vascular barrier controls the systemic dissemination of bacteria. Science (New York, NY). 2015;350(6262):830-4.
2. Brescia P, Rescigno M. The gut vascular barrier: a new player in the gut–liver–brain axis. Trends in Molecular Medicine. 2021;27(9):844-55.
3. Ghosh S, Whitley CS, Haribabu B, Jala VR. Regulation of Intestinal Barrier Function by Microbial Metabolites. Cellular and Molecular Gastroenterology and Hepatology. 2021;11(5):1463-82.
4. Zhao Y, Chen F, Wu W, Sun M, Bilotta AJ, Yao S, et al. GPR43 mediates microbiota metabolite SCFA regulation of antimicrobial peptide expression in intestinal epithelial cells via activation of mTOR and STAT3. Mucosal immunology. 2018;11(3):752-62.
5. Schulthess J, Pandey S, Capitani M, Rue-Albrecht KC, Arnold I, Franchini F, et al. The short chain fatty acid butyrate imprints an antimicrobial program in macrophages. Immunity. 2019;50(2):432-45. e7.
6. Hajra D, Kirthivasan N, Chakravortty D. Symbiotic Synergy from Sponges to Humans: Microflora-Host Harmony Is Crucial for Ensuring Survival and Shielding against Invading Pathogens. ACS infectious diseases. 2024;10(2):317-36.
7. Garcia-del Portillo F, Foster JW, Finlay BB. Role of acid tolerance response genes in Salmonella typhimurium virulence. Infection and immunity. 1993;61(10):4489-92.
8. Haraga A, Ohlson MB, Miller SI. Salmonellae interplay with host cells. Nat Rev Microbiol. 2008;6(1):53-66.
9. Hensel M. Evolution of pathogenicity islands of Salmonella enterica. International journal of medical microbiology : IJMM. 2004;294(2-3):95-102.
10. Hajra D. Understanding the mechanism of host deacetylase SIRT1 and SIRT3 in the modulation of Salmonella pathogenesis. 2024.
11. Wang J, Lang T, Shen J, Dai J, Tian L, Wang X. Core Gut Bacteria Analysis of Healthy Mice. Frontiers in microbiology. 2019;10:887.

12. Hiippala K, Barreto G, Burrello C, Diaz-Basabe A, Suutarinen M, Kainulainen V, et al. Novel Odoribacter splanchnicus Strain and Its Outer Membrane Vesicles Exert Immunoregulatory Effects in vitro. Frontiers in microbiology. 2020;11:575455.
13. Xing C, Wang M, Ajibade AA, Tan P, Fu C, Chen L, et al. Microbiota regulate innate immune signaling and protective immunity against cancer. Cell host & microbe. 2021;29(6):959-74.e7.
14. Gogoi M, Chandra K, Sarikhani M, Ramani R, Sundaresan NR, Chakravortty D. Salmonella escapes adaptive immune response via SIRT2 mediated modulation of innate immune response in dendritic cells. PLoS pathogens. 2018;14(11):e1007437.
15. Schaefer JS, Montufar-Solis D, Nakra N, Vigneswaran N, Klein JR. Small intestine inflammation in Roquin-mutant and Roquin-deficient mice. PloS one. 2013;8(2):e56436.
16. Erben U, Loddenkemper C, Doerfel K, Spieckermann S, Haller D, Heimesaat MM, et al. A guide to histomorphological evaluation of intestinal inflammation in mouse models. International journal of clinical and experimental pathology. 2014;7(8):4557-76.
17. Hajra D, Nair AV, Roy Chowdhury A, Mukherjee S, Chatterjee R, Chakravortty D. Salmonella Typhimurium U32 peptidase, YdcP, promotes bacterial survival by conferring protection against in vitro and in vivo oxidative stress. Microbial pathogenesis. 2022;173(Pt B):105862.
18. Roy Chowdhury A, Hajra D, Mukherjee D, Nair AV, Chakravortty D. Functional OmpA of Salmonella Typhimurium provides protection from lysosomal degradation and inhibits autophagic processes in macrophages. The Journal of infectious diseases. 2024.
19. Chandra K, Nair AV, Chatterjee R, Muralidhara P, Singh A, Kamanna S, et al. Absence of proline-peptide transporter YjiY in Salmonella Typhimurium leads to secretion of factors which inhibits intra-species biofilm formation. Microbiological research. 2023;273:127411.
20. Hajra D, Rajmani RS, Chaudhary AD, Gupta SK, Chakravortty D. Salmonella-induced SIRT1 and SIRT3 are crucial for maintaining the metabolic switch in bacteria and host for successful pathogenesis. eLife Sciences Publications, Ltd; 2024.
21. Balakrishnan A, Schnare M, Chakravortty D. Of men not mice: bactericidal/permeability-increasing protein expressed in human macrophages acts as a phagocytic receptor and modulates entry and replication of Gram-negative bacteria. Frontiers in immunology. 2016;7:455.
22. Chatterjee R, Chowdhury AR, Nair AV, Hajra D, Kar A, Datey A, et al. Salmonella Typhimurium PgtE is an essential arsenal to defend against the host resident antimicrobial peptides. Microbiological research. 2023;271:127351.
23. Goubier A, Dubois B, Gheit H, Joubert G, Villard-Truc F, Asselin-Paturel C, et al. Plasmacytoid Dendritic Cells Mediate Oral Tolerance. Immunity. 2008;29(3):464-75.
24. Müller-Redetzky HC, Suttorp N, Witzenrath M. Dynamics of pulmonary endothelial barrier function in acute inflammation: mechanisms and therapeutic perspectives. Cell and tissue research. 2014;355(3):657-73.
25. Daneman R, Rescigno M. The gut immune barrier and the blood-brain barrier: are they so different? Immunity. 2009;31(5):722-35.
26. Yuan SY, Rigor RR. Integrated Systems Physiology: From Molecule to Function to Disease. Regulation of Endothelial Barrier Function. San Rafael (CA): Morgan & Claypool Life Sciences

Copyright © 2011 by Morgan & Claypool Life Sciences.; 2010.

27. Wang Y, Rattner A, Zhou Y, Williams J, Smallwood PM, Nathans J. Norrin/Frizzled4 signaling in retinal vascular development and blood brain barrier plasticity. Cell. 2012;151(6):1332-44.
28. Liebner S, Corada M, Bangsow T, Babbage J, Taddei A, Czupalla CJ, et al. Wnt/beta-catenin signaling controls development of the blood-brain barrier. The Journal of cell biology. 2008;183(3):409-17.
29. Oehlers SH, Cronan MR, Scott NR, Thomas MI, Okuda KS, Walton EM, et al. Interception of host angiogenic signalling limits mycobacterial growth. Nature. 2015;517(7536):612-5.
30. Iwase T, Uehara Y, Shinji H, Tajima A, Seo H, Takada K, et al. Staphylococcus epidermidis Esp inhibits Staphylococcus aureus biofilm formation and nasal colonization. Nature. 2010;465(7296):346-9.

31. Lee J, Jayaraman A, Wood TK. Indole is an inter-species biofilm signal mediated by SdiA. BMC microbiology. 2007;7(1):1-15.
32. Fux CA, Costerton JW, Stewart PS, Stoodley P. Survival strategies of infectious biofilms. Trends in microbiology. 2005;13(1):34-40.
33. Costerton JW, Stewart PS, Greenberg EP. Bacterial biofilms: a common cause of persistent infections. Science (New York, NY). 1999;284(5418):1318-22.
34. Hajra D, Nair AV, Chakravortty D. An elegant nano-injection machinery for sabotaging the host: Role of Type III secretion system in virulence of different human and animal pathogenic bacteria. Physics of life reviews. 2021;38:25-54.
35. Jennings ME, Quick LN, Ubol N, Shrom S, Dollahon N, Wilson JW. Characterization of Salmonella type III secretion hyper-activity which results in biofilm-like cell aggregation. PloS one. 2012;7(3):e33080.
36. Ducarmon QR, Zwittink RD, Hornung BVH, van Schaik W, Young VB, Kuijper EJ. Gut Microbiota and Colonization Resistance against Bacterial Enteric Infection. Microbiology and molecular biology reviews : MMBR. 2019;83(3).
37. Caballero-Flores G, Pickard JM, Núñez G. Microbiota-mediated colonization resistance: mechanisms and regulation. Nature Reviews Microbiology. 2023;21(6):347-60.
38. Qin J, Li R, Raes J, Arumugam M, Burgdorf KS, Manichanh C, et al. A human gut microbial gene catalogue established by metagenomic sequencing. Nature. 2010;464(7285):59-65.
39. Gewolb IH, Schwalbe RS, Taciak VL, Harrison TS, Panigrahi P. Stool microflora in extremely low birthweight infants. Archives of disease in childhood Fetal and neonatal edition. 1999;80(3):F167-73.
40. Chakraborty P, Bajeli S, Kaushal D, Radotra BD, Kumar A. Biofilm formation in the lung contributes to virulence and drug tolerance of Mycobacterium tuberculosis. Nature communications. 2021;12(1):1606.
41. Yamamoto K, Tsujimura Y, Ato M. Catheter-associated Mycobacterium intracellulare biofilm infection in C3HeB/FeJ mice. Sci Rep. 2023;13(1):17148.
42. Heilbronner S, Krismer B, Brötz-Oesterhelt H, Peschel A. The microbiome-shaping roles of bacteriocins. Nature reviews Microbiology. 2021;19(11):726-39.
43. Cotter PD, Ross RP, Hill C. Bacteriocins - a viable alternative to antibiotics? Nature reviews Microbiology. 2013;11(2):95-105.
44. Watson KG, Holden DW. Dynamics of growth and dissemination of Salmonella in vivo. Cellular microbiology. 2010;12(10):1389-97.
45. McGuckin MA, Lindén SK, Sutton P, Florin TH. Mucin dynamics and enteric pathogens. Nature reviews Microbiology. 2011;9(4):265-78.
46. Eberl C, Weiss AS, Jochum LM, Durai Raj AC, Ring D, Hussain S, et al. E. coli enhance colonization resistance against Salmonella Typhimurium by competing for galactitol, a context-dependent limiting carbon source. Cell host & microbe. 2021;29(11):1680-92.e7.
47. Litvak Y, Mon KKZ, Nguyen H, Chanthavixay G, Liou M, Velazquez EM, et al. Commensal Enterobacteriaceae Protect against Salmonella Colonization through Oxygen Competition. Cell host & microbe. 2019;25(1):128-39.e5.
48. Oliveira RA, Ng KM, Correia MB, Cabral V, Shi H, Sonnenburg JL, et al. Klebsiella michiganensis transmission enhances resistance to Enterobacteriaceae gut invasion by nutrition competition. Nat Microbiol. 2020;5(4):630-41.
49. Chanda D, De D. Meta-analysis reveals obesity associated gut microbial alteration patterns and reproducible contributors of functional shift. Gut Microbes. 2024;16(1):2304900.
50. Lima SF, Gogokhia L, Viladomiu M, Chou L, Putzel G, Jin WB, et al. Transferable Immunoglobulin A-Coated Odoribacter splanchnicus in Responders to Fecal Microbiota Transplantation for Ulcerative Colitis Limits Colonic Inflammation. Gastroenterology. 2022;162(1):166-78.

853 51. Kommineni S, Bretl DJ, Lam V, Chakraborty R, Hayward M, Simpson P, et al. Bacteriocin
854 production augments niche competition by enterococci in the mammalian gastrointestinal tract.
855 Nature. 2015;526(7575):719-22.
856 52. Kommineni S, Kristich CJ, Salzman NH. Harnessing bacteriocin biology as targeted therapy in
857 the GI tract. Gut Microbes. 2016;7(6):512-7.
858 53. Lawrence GW, McCarthy N, Walsh CJ, Kunyoshi TM, Lawton EM, O'Connor PM, et al. Effect of
859 a bacteriocin-producing Streptococcus salivarius on the pathogen Fusobacterium nucleatum in a
860 model of the human distal colon. Gut Microbes. 2022;14(1):2100203.
861 54. Heeney DD, Zhai Z, Bendiks Z, Barouei J, Martinic A, Slupsky C, et al. Lactobacillus plantarum
862 bacteriocin is associated with intestinal and systemic improvements in diet-induced obese mice and
863 maintains epithelial barrier integrity in vitro. Gut Microbes. 2019;10(3):382-97.
864 55. Kuniyoshi TM, O'Connor PM, Lawton E, Thapa D, Mesa-Pereira B, Abulu S, et al. An oxidation
865 resistant pediocin PA-1 derivative and penocin A display effective anti-Listeria activity in a model
866 human gut environment. Gut Microbes. 2022;14(1):2004071.
867 56. Hajra D, Mukherjee D, Vij R, Rajmani RS, Dadireddy V, Das D, et al. Odoribacter splanchnicus
868 mitigates Salmonella-induced gut inflammation and its associated pathogenesis via its secreted
869 bacteriocin. bioRxiv. 2024:2024.08.23.609322.

870
871

872 **MAIN FIGURES AND LEGENDS**

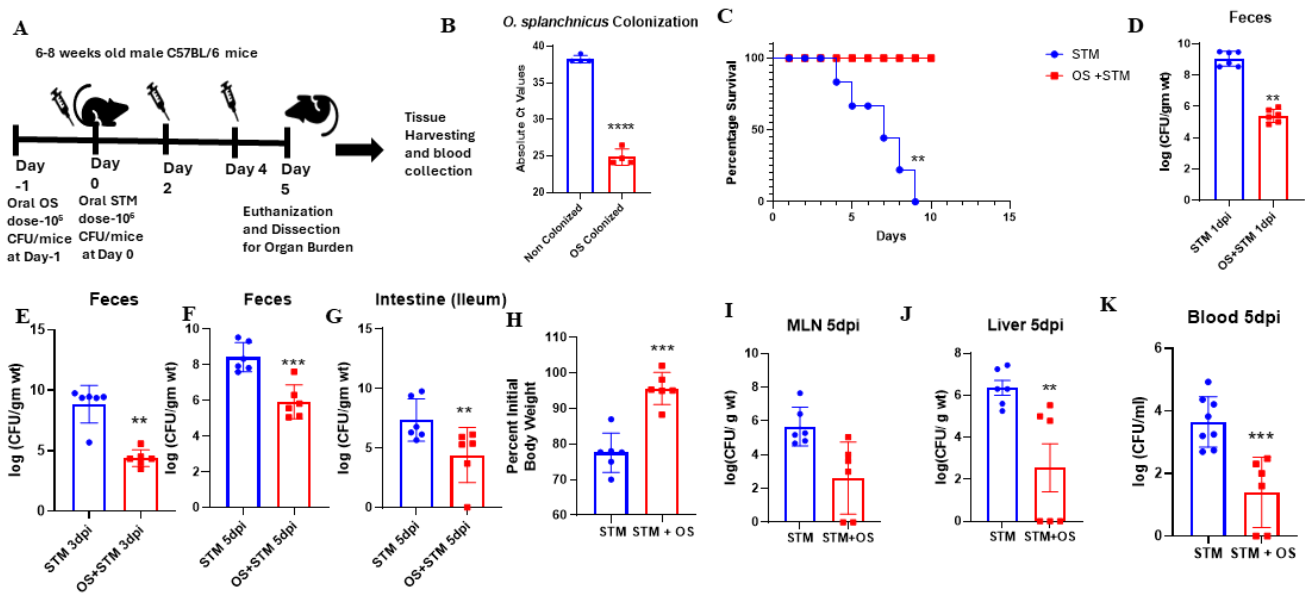

873

874 **Figure 1. *Odoribacter splanchnicus* colonization protects mice from *Salmonella***
875 **colonization and dissemination**

876 **A**-Schematic representation showing animal experimental strategy of infection.

877 **B**-OS colonization validation via qPCR quantification of *O. splanchnicus* 16S rRNA from fecal
878 samples of mice at 6th day post-OS colonization .

879 **C**-Survival percentage of non-colonized-STM-infected mice versus OS-colonized-STM-
880 infected mice cohorts. Data is representative of N=3, n=5 where N denotes number of
881 biological replicates and n denotes the number of mice per group. Mantel Cox or the log-rank
882 test was used to determine the p values.

883 **D-G**- STM organ loads in feces at 1st day post-infection (D), 3rd day post-infection (E), 5th
884 post-infection (F) and in ileal tissues (contents and wall) at 5th day post-infection (G) in OS
885 colonized and non-colonized mice cohorts. Data is representative of N=2, n=6 where N
886 denotes number of biological replicates and n denotes the number of mice per group. Mann
887 Whitney Test was performed to obtain p-values.

888 **H**-Percent of initial weight (at Day 0) exhibited by OS colonized and non-colonized mice upon
889 STM infection at 5th day post-infection. Data is representative of N=3,n=6 where N denotes
890 number of biological replicates and n denotes the number of mice per group.

891 **I-K**- STM organ loads in MLN (I), liver (J) and blood (K) at 5th post-infection in OS colonized
892 and non-colonized mice cohorts. Data is representative of N=3, n=6 where N denotes number
893 of biological replicates and n denotes the number of mice per group. Mann Whitney Test was
894 performed to obtain p-values.

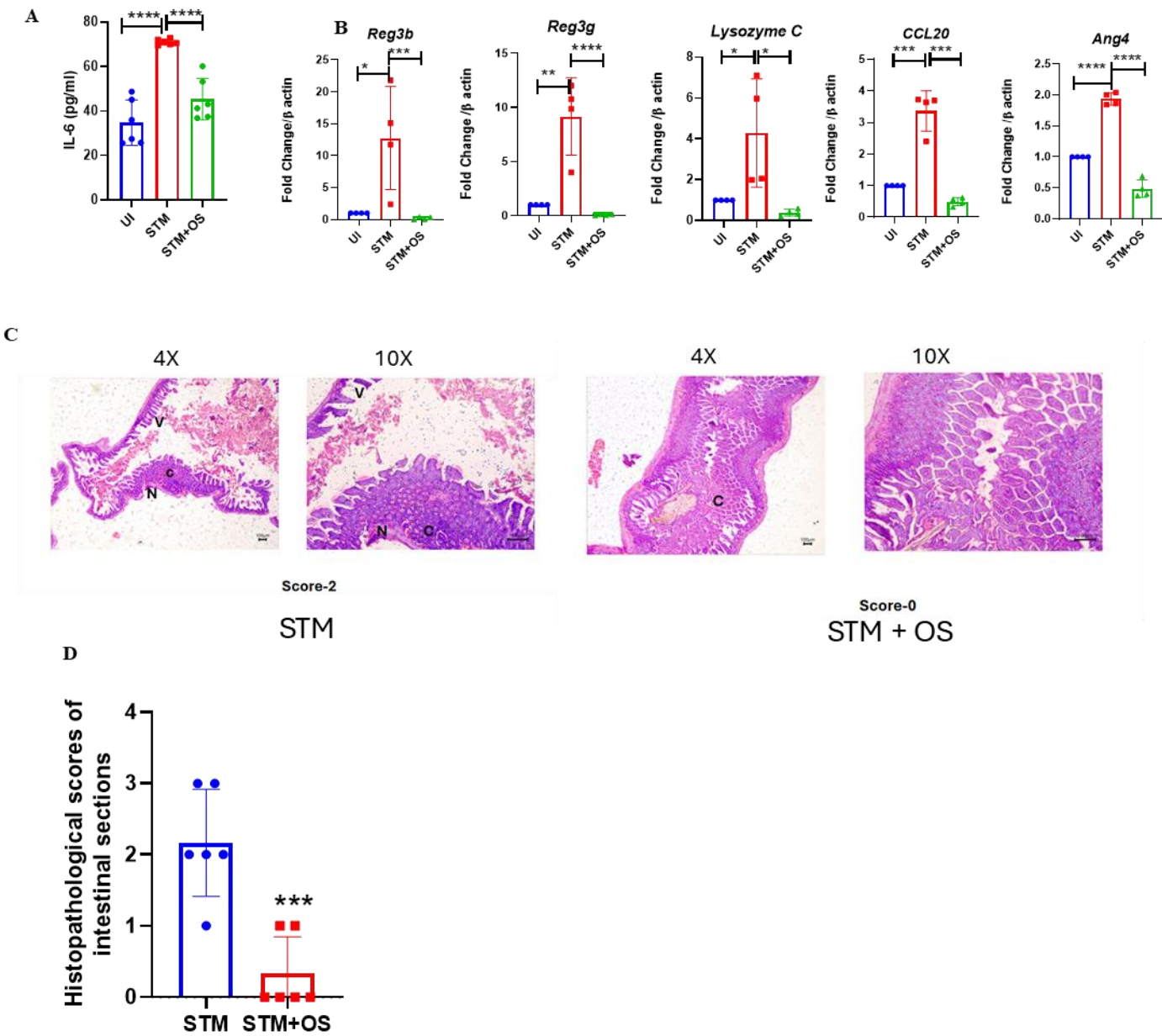

Figure 2. *O. splanchnicus* reduces *Salmonella*-induced inflammation and intestinal damage

A-Estimation of serum IL-6 production via ELISA upon STM infection in OS non-colonized and colonized mice cohorts at 5th day post-*Salmonella* infection. Unpaired t-test is performed to obtain the p-values. Data is representative of N=3, n=3.

901 **B**-Quantitative gene expression data of several antimicrobial peptides (AMPs) precursor genes
902 in uninfected (UI) and STM-infected mice intestinal tissues harvested at 5th dpi from OS
903 colonized or non-colonized cohorts. Unpaired t-test is performed to obtain the p-values. Data
904 is representative of N=3, n=4.

905 **C- D**-Haematoxylin-eosin-stained intestinal sections harvested from STM-infected OS non-
906 colonized or colonized mice cohorts at 5th dpi. 0-represents normal pathology, 1- represents-
907 mild pathology, 2-3-represents severe pathology.

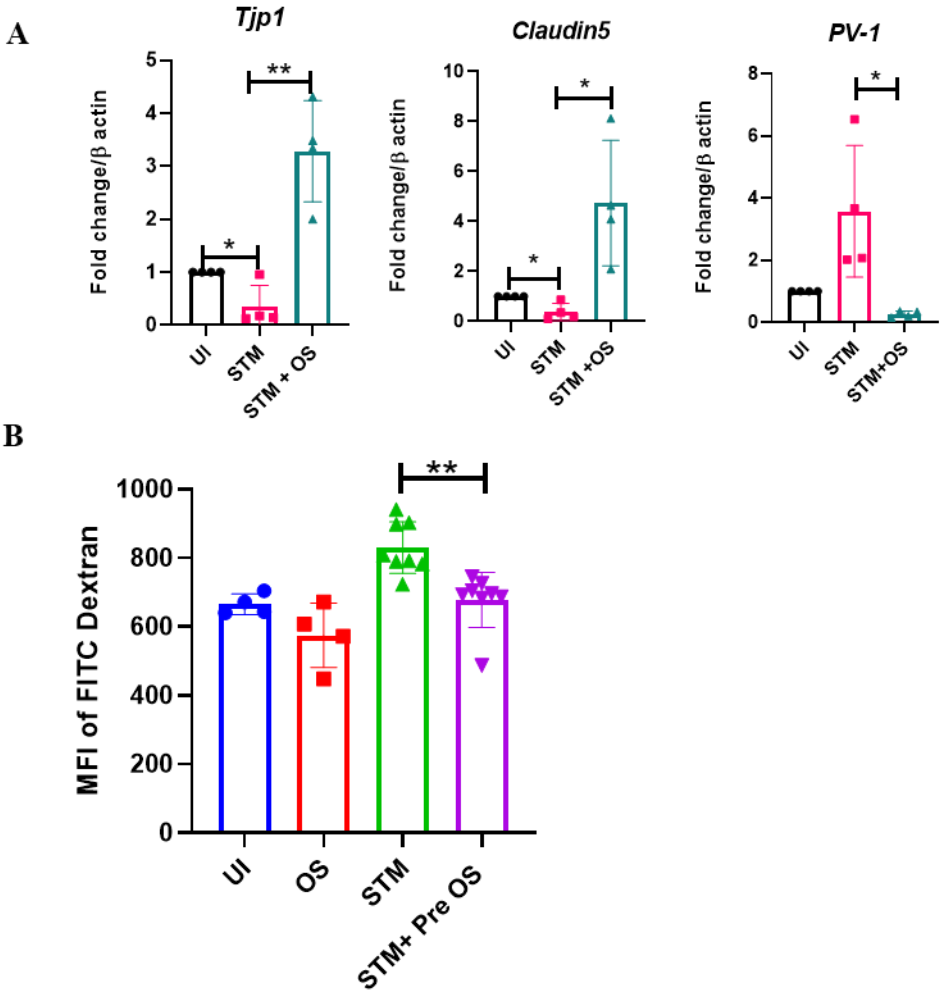

908

909 **Fig 3. *Odoribacter splanchnicus* gut colonization prevents *Salmonella*-induced GVB**
910 **damage and promotes tight junction gene expression.**

911 **A**-Quantitative gene expression studies of tight junction protein complexes (*Tjp1*, *Claudin5*)
912 and PV-1 gene (marker of GVB damage) in STM-infected mice intestinal (ileal) tissue in
913 presence or absence of OS gut colonization at 5th day post-infection. Un-paired t-test was used
914 to obtain the p-values. Data is representative of N=3, n=4.

915 **B**- Estimation of FITC fluorescence in mice plasma via gut permeability assay in infected mice
916 cohorts upon oral administration of FITC Dextran (25mg/kg) 4h before euthanization at 5th day
917 post *Salmonella* infection. Un-paired t-test was used to obtain the p-values. Data is
918 representative of N=4.

919

920

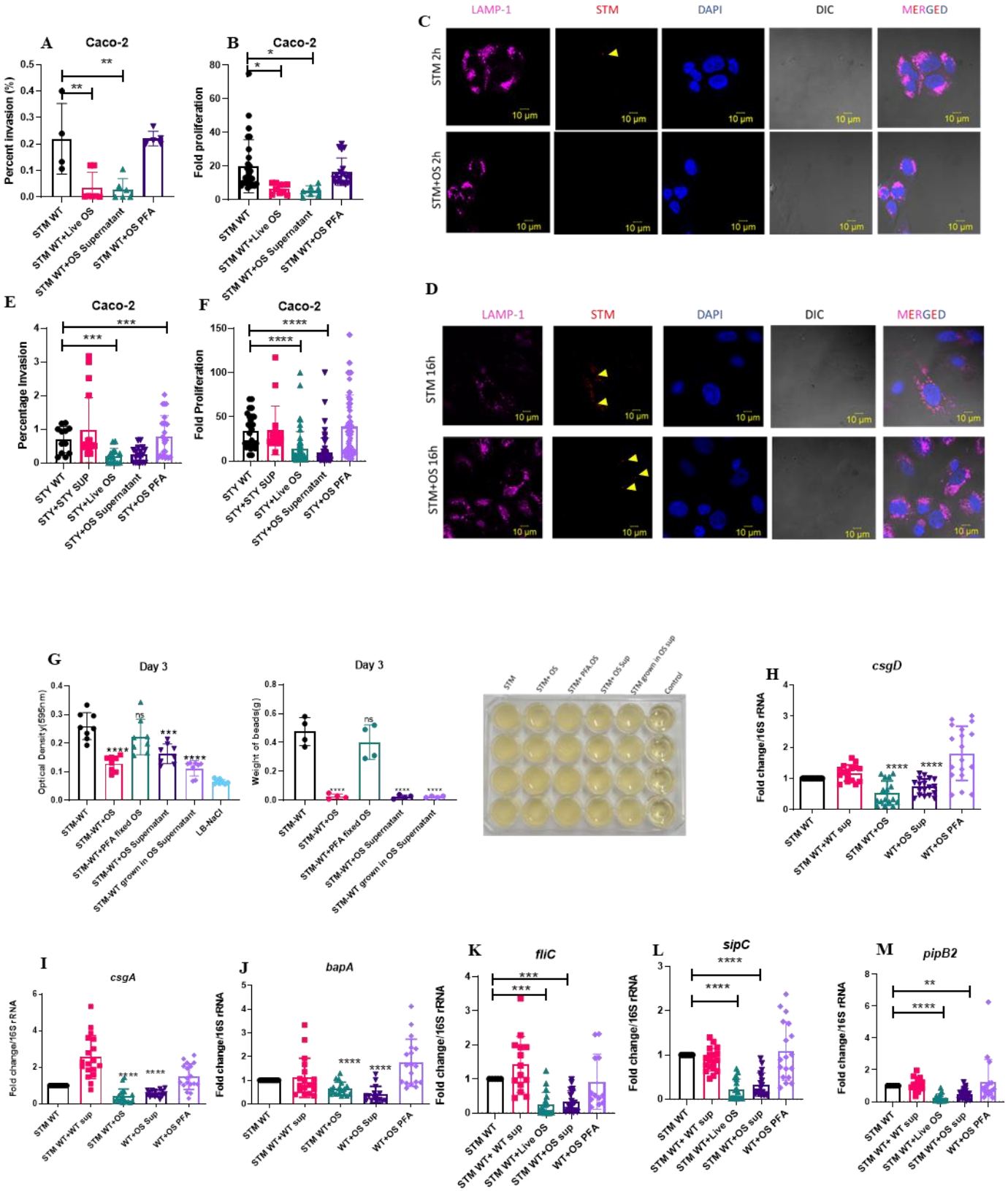
A
Caco-2
Percent invasion (%)
STM WT
STM WT+Live OS
STM WT+OS Supernatant
STM WT+OS PFA
B
Caco-2
Fold proliferation
C
LAMP-1
STM
DAPI
DIC
MERGED
STM 2h
STM+OS 2h
10 µm
D
STM 16h
STM+OS 16h
E
Caco-2
Percentage Invasion
STY WT
STY+STY SUP
STY+Live OS
STY+OS Supernatant
STY+OS PFA
F
Caco-2
Fold Proliferation
G
Day 3
Optical Density(595nm)
STM-WT
STM-WT+OS
STM-WT+PFA fixed OS
STM-WT+OS Supernatant
STM-WT grown in OS Supernatant
LB-NaCl
Day 3
Weight of beads(g)
STM
STM+ OS
STM+ PFA OS
STM+ OS Sup
STM grown in OS sup
Control
H
csgD
Fold change/16S rRNA
STM WT
STM WT+WT sup
STM WT+OS
WT+OS Sup
WT+OS PFA
I
csgA
J
bapA
K
fliC
STM WT+ WT sup
STM WT+Live OS
STM WT+OS sup
L
sipC
M
pipB2

921

922

923

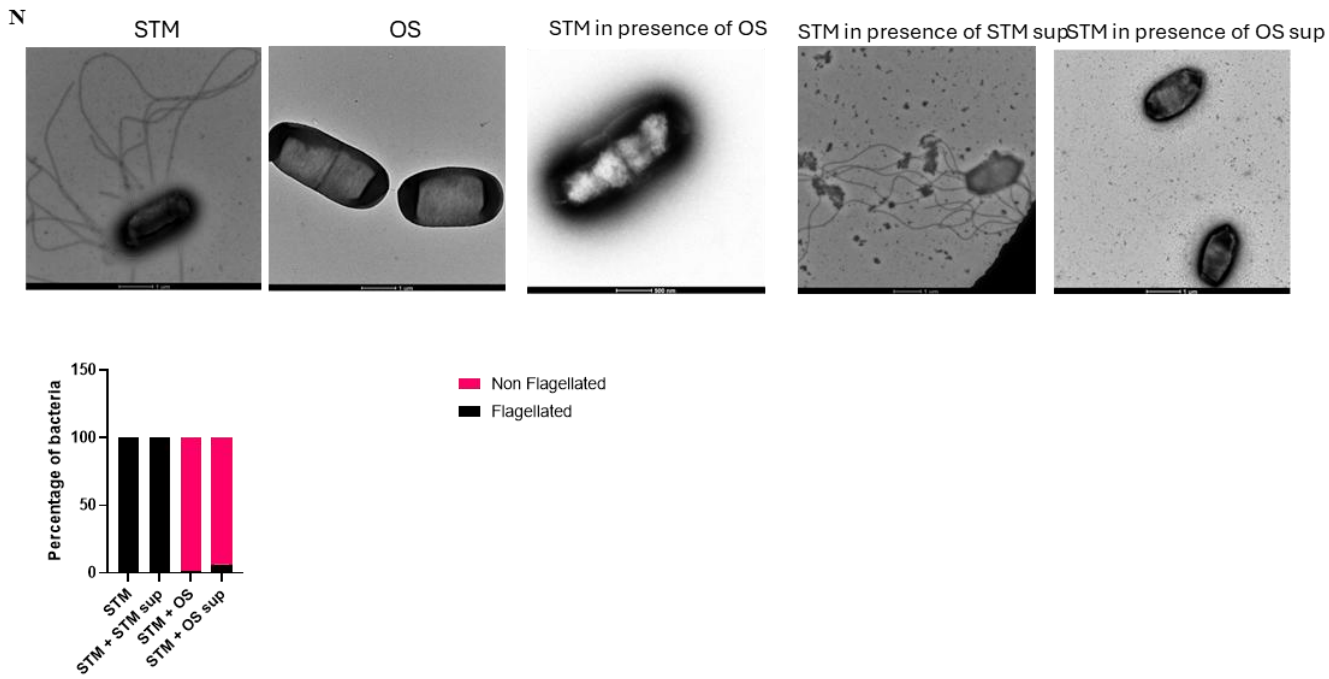

Fig 4. *O. splanchnicus* exhibits its inhibitory effect on *Salmonella* biofilm formation and inhibits invasion and intracellular replication in human intestinal cells

A-Percent invasion of STM in human Caco-2 human intestinal cells in presence or absence of live OS, OS culture supernatant, PFA-fixed-OS. Data is representative of N=3, n=4. One-way ANOVA was used to determine the p-values.

B-Intracellular proliferation of STM Caco-2 cells in presence or absence of live OS, OS culture supernatant, PFA-fixed-OS. Data is representative of N=3, n=4. One-way ANOVA was used to determine the p-values.

937 **C**- Representative immunofluorescence images depicting STM invasion into Caco-2 cells in
938 the presence or absence of OS at 2hr post-infection. Data is representative of N=3, n=100.

939 **D**- Representative immunofluorescence images depicting STM invasion into Caco-2 cells in
940 presence or absence of OS at 2hr post-infection. Data is representative of N=3, n=100.

941 **E**-Percent invasion of STY in Caco-2 human cells in presence or absence of OS, OS culture
942 supernatant, PFA-fixed OS. Data is representative of N=3, n≥9. One-way ANOVA was used to
943 determine the p-values.

944 **F**-Intracellular proliferation of STY in Caco-2 cells in presence or absence of live OS, OS
945 culture supernatant, PFA-fixed-OS. Data is representative of N=3, n≥9. One-way ANOVA was
946 used to determine the p-values.

947 **G**- Biofilm assay showing the biofilm formation ability of STM-WT or STM-WT grown in OS
948 supernatant after 72h of inoculation in presence or absence of live OS, OS culture supernatant,
949 PFA-fixed-OS. Data is representative of N=4, n=4.One-way ANOVA was used to determine
950 the p-values. Image of the STM biofilm-formed plate in the above stated conditions has been
951 shown.

952 **H-M-** RT-qPCR mediated gene expression of STM biofilm regulatory genes (*csgD*) (H), *csgA*
953 (I), *bapA* (J), along with flagellar gene (*fliC*) (K), SPI-1 (*sipC*) (L) and SPI-2 (*pipB2*) (M)
954 genes in presence or absence of live OS or its spent media or PFA-fixed-OS. Data is
955 representative of N=4, n=4. One-way ANOVA was used to determine the p-values.

956 **N-** Transmission Electron Microscopic (TEM) images of STM in presence or absence of
957 *Salmonella* WT supernatant, OS and its supernatant to assess the possession of flagella. The
958 quantification plot exhibits the percentage of bacterial flagellated or non-flagellated cells
959 (number of cells quantified n≥ 100)

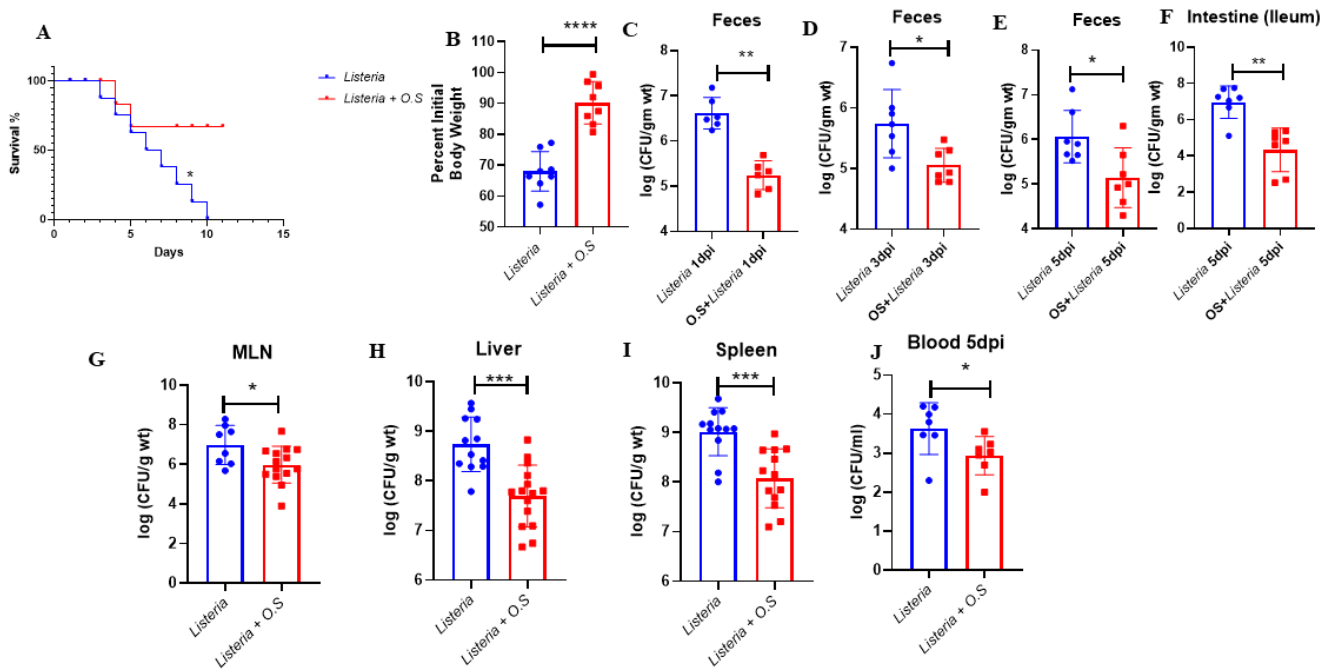

Fig 5. *Odoribacter splanchnicus* exerts its protective role against *Listeria monocytogenes* in mice

A- Survival percentage of non-colonized LM-infected mice versus OS-colonized *Listeria*-infected mice cohorts. Data is represantative of N=2, n=8, where N denotes number of biological replicates and n denotes the number of mice per group. Mantel Cox or the log-rank test was used to determine the p values.

B-Percent of initial weight (at Day 0) exhibited by OS colonized and non-colonized mice upon LM infection at 5th dpi. Data is representative of N=2,n=8, where N denotes number of biological replicates and n denotes the number of mice per group. Mann Whitney Test was performed to obtain p-values.

973 **C-F**- LM organ loads in feces at 1st day post-infection (C), 3rd day post-infection (D), 5th post-
974 infection (E) and in ileal tissues (contents and wall) at 5th day post-infection (F) in OS pre-
975 colonized and non-colonized mice cohorts. Data is representative of N=2, n=7 where N
976 denotes number of biological replicates and n denotes the number of mice per group. Mann
977 Whitney Test was performed to obtain p-values.

978 **G-J**- LM organ loads in Mesenteric lymph Node (MLN) (G), liver (H), spleen (I) and blood
979 (J) at 5th dp. in OS colonized and non-colonized mice cohorts Data is representative of N=2,
980 n=8, where N denotes number of biological replicates and n denotes the number of mice per
981 group. Mann Whitney Test was performed to obtain p-values.

982

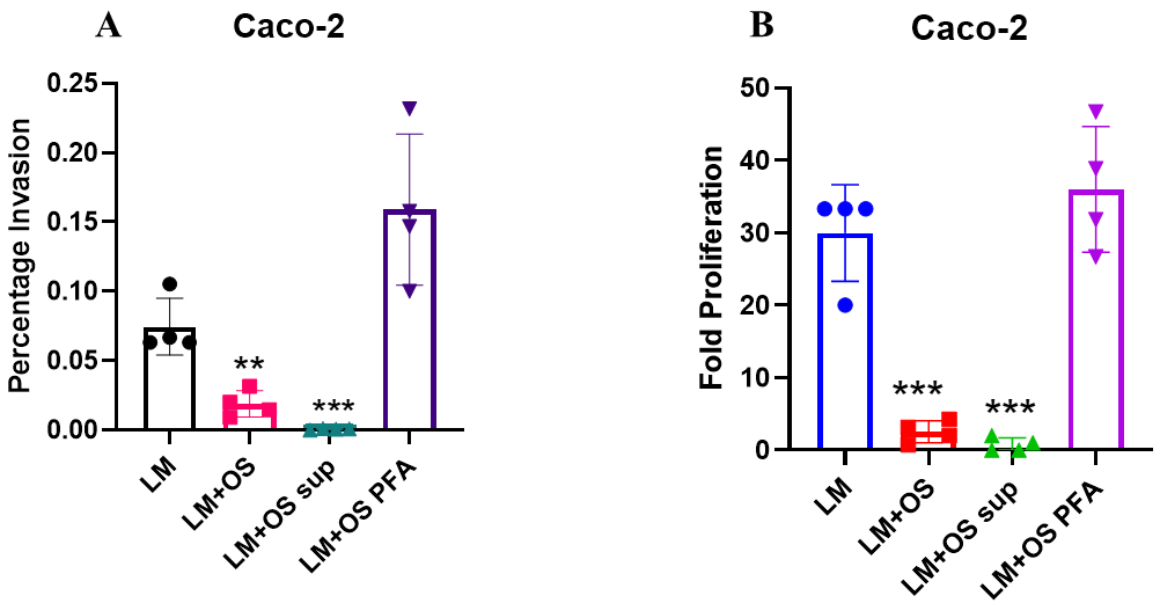

983

984 **Fig. 6 *Odoribacter splanchnicus* and its culture supernatant restricts *Listeria***
985 ***monocytogenes* pathogenesis in human intestinal cells**

986 **A**- Percent invasion of LM in Caco-2 cells in presence or absence of live OS, OS sup, PFA-
987 fixed-OS. Data is representative of N=3, n=4. One-way ANOVA and Multiple Comparison test
988 are used to obtain the p-values.

989 **B**-Intracellular fold proliferation of LM in Caco-2 cells in the presence or absence of live OS,
990 OS sup, PFA-fixed-OS. Data is representative of N=3, n=4. One-way ANOVA and Multiple
991 Comparison test are used to obtain the p-values.

992

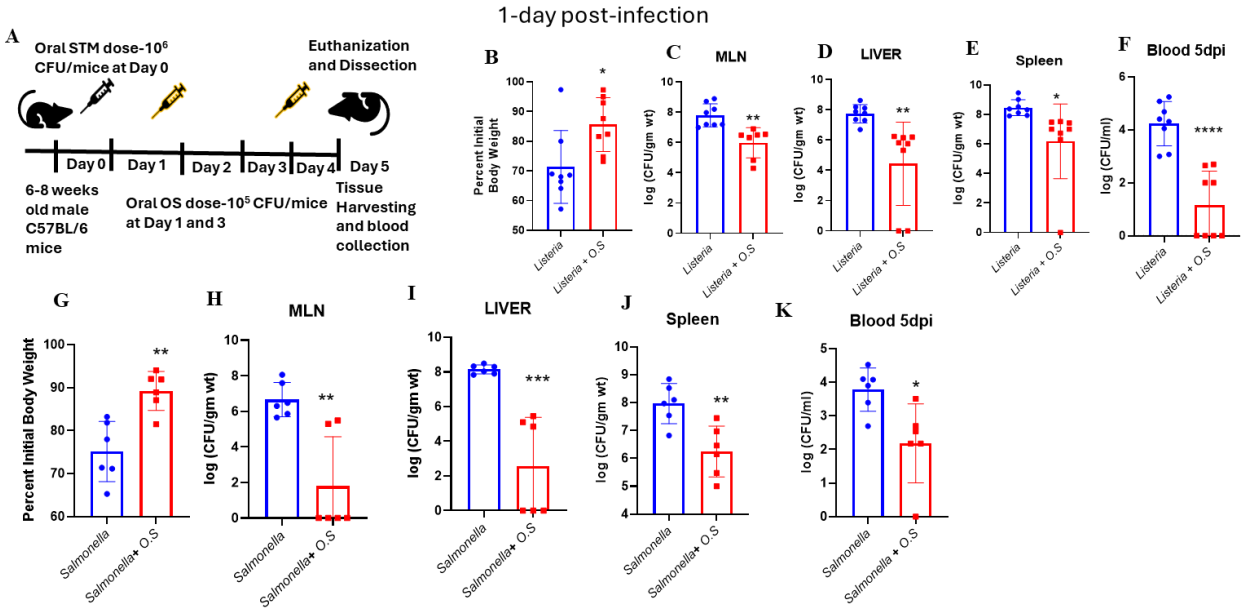

993

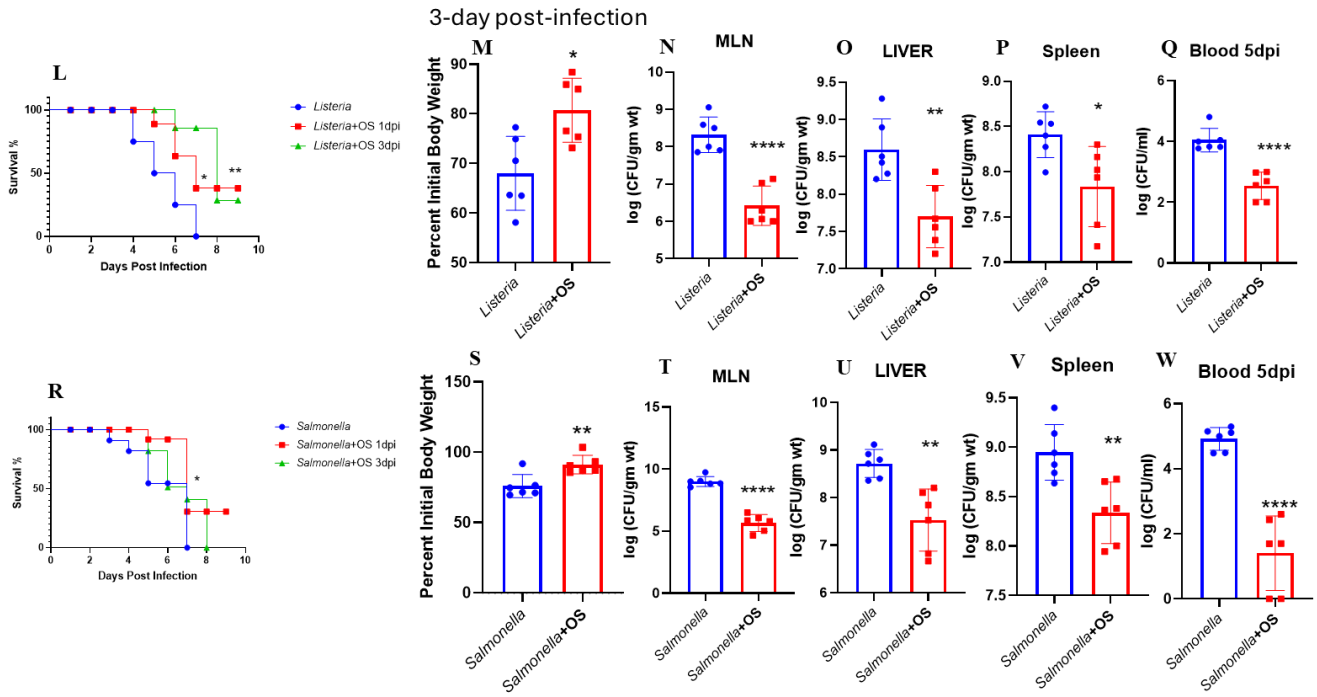

Fig. 7 *O. splanchnicus* even confers protection against foodborne pathogens when administered post-pathogenic challenge

A- Schematic representation showing the animal experimental strategy of infection.

B- Percent of initial weight (at Day 0) exhibited by OS colonized (1-dpi) and non-colonized mice upon LM infection at 5th dpi. Data is representative of N=2,n=8, where N denotes number of biological replicates and n denotes the number of mice per group. Mann Whitney Test was performed to obtain p-values.

C-F- LM organ loads in MLN (C), liver (D), spleen (E) and blood (F) at 5th dpi upon OS administration at 1-dpi. Data is representative of N=2, n=8, where N denotes number of biological replicates and n denotes the number of mice per group. Mann Whitney Test was performed to obtain p-values.

1008 **G**- Percent of initial weight (at Day 0) exhibited by OS colonized (1-dpi) and non-colonized
1009 mice upon STM infection at 5th dpi. Data is representative of N=2,n=8, where N denotes
1010 number of biological replicates and n denotes the number of mice per group. Mann Whitney
1011 Test was performed to obtain p-values.

1012 **H-K**- STM organ loads in MLN (H), liver (I), spleen (J) and blood (K) at 5th-dpi upon OS
1013 administration at 1-dpi. Data is representative of N=2, n=8, where N denotes number of
1014 biological replicates and n denotes the number of mice per group. Mann-Whitney Test was
1015 performed to obtain p-values.

1016 **L**- Survival percentage of non-colonized LM-infected mice versus OS-colonized (1 dpi or 3
1017 dpi) *Listeria*-infected mice cohorts. Data is representative of N=2, n=8, where N denotes
1018 number of biological replicates and n denotes the number of mice per group. Mantel Cox or
1019 the log-rank test was used to determine the p values.

1020 **M**- Percent weight loss exhibited by OS colonized (3-dpi) and non-colonized mice upon LM
1021 infection at 5th-day post-infection. Data is representative of N=2,n=8, where N denotes number
1022 of biological replicates and n denotes the number of mice per group.Mann-Whitney Test was
1023 performed to obtain p-values.

1024

1025 **N-Q**- LM organ loads in MLN (N), liver (O), spleen (P) and blood (Q) at 5th-dpi upon OS
1026 administration at 3-dpi. Data is representative of N=2, n=8, , where N denotes number of
1027 biological replicates and n denotes the number of mice per group. Mann-Whitney Test was
1028 performed to obtain p-values.

1029 **R**- Survival percentage of non-colonized *Salmonella*-infected mice versus OS-colonized (1 dpi
1030 or 3 dpi) *Listeria*-infected mice cohorts. Data is represantative of N=2, n=8, where N denotes

1031 number of biological replicates and n denotes the number of mice per group. Mantel Cox or
1032 the log-rank test was used to determine the p values.

1033 **S**- Percent weight loss exhibited by OS-colonized (3-dpi) and non-colonized mice upon STM
1034 infection at 5th-day post-infection. Data is representative of N=2,n=8, where N denotes number
1035 of biological replicates and n denotes the number of mice per group. Mann-Whitney Test was
1036 performed to obtain p-values.

1037 **T-W**-STM organ loads in MLN (T), liver (U), spleen (V), and blood (W) at 5th-dpi upon OS
1038 administration at 3-dpi. Data is representative of N=2, n=8, where N denotes number of
1039 biological replicates and n denotes the number of mice per group. Mann-Whitney Test was
1040 performed to obtain p-values.

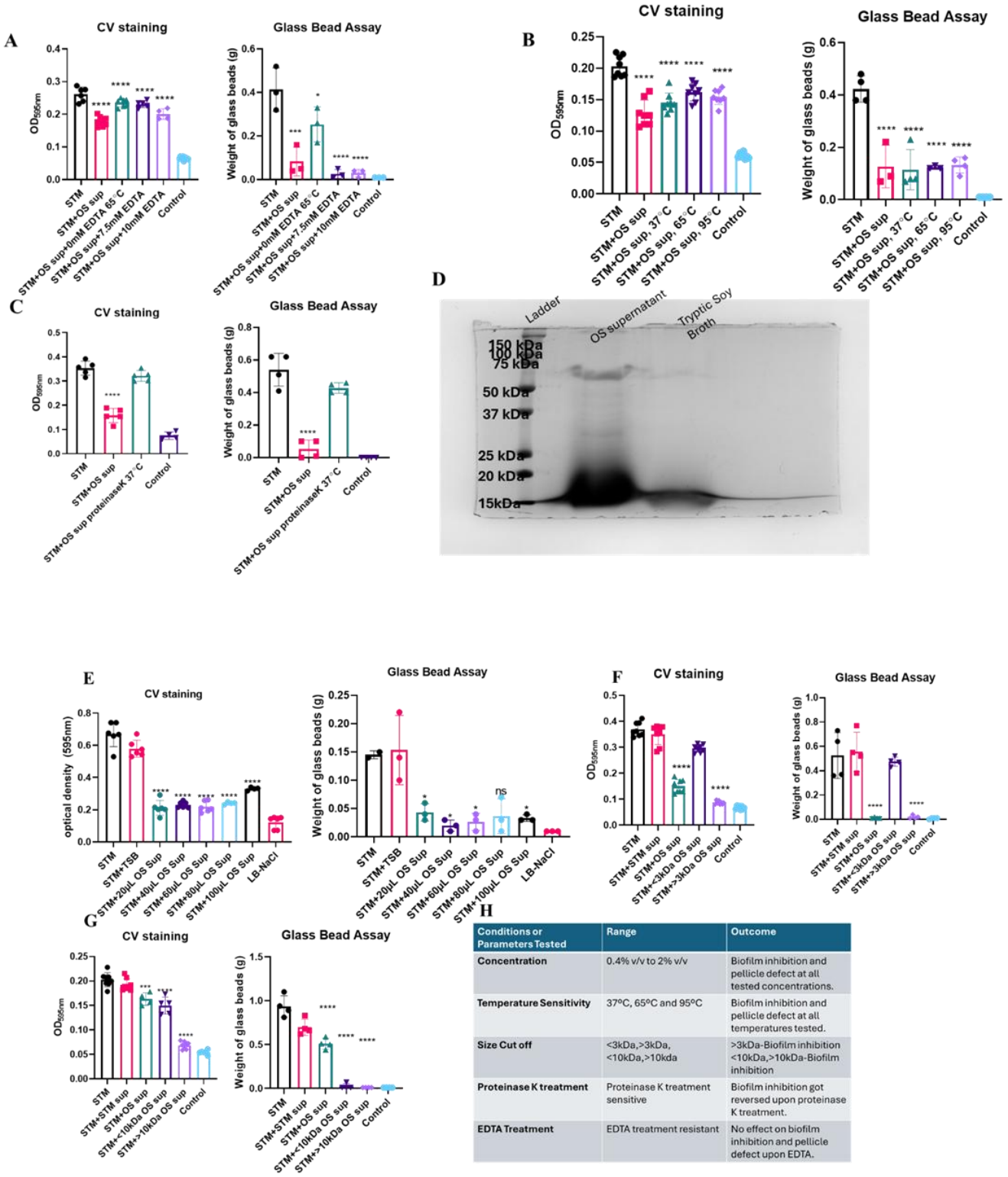

H

Conditions or Parameters Tested	Range	Outcome
Concentration	0.4% v/v to 2% v/v	Biofilm inhibition and pellicle defect at all tested concentrations.
Temperature Sensitivity	37°C, 65°C and 95°C	Biofilm inhibition and pellicle defect at all temperatures tested.
Size Cut off	<3kDa,>3kDa, <10kDa,>10kda	>3kDa-Biofilm inhibition <10kDa,>10kDa-Biofilm inhibition
Proteinase K treatment	Proteinase K treatment sensitive	Biofilm inhibition got reversed upon proteinase K treatment.
EDTA Treatment	EDTA treatment resistant	No effect on biofilm inhibition and pellicle defect upon EDTA.

Fig. 8- Characterization of the nature of inhibitory active molecule within *O. splanchnicus* culture supernatant

1045 **A-** Biofilm assay showing the biofilm formation ability of STM after 72h of inoculation in
1046 presence of OS culture supernatant upon EDTA treatment. Data is representative of N=4, n=4.
1047 One-way ANOVA is used to obtain the p-values. Statistical test is performed with respect to
1048 STM.

1049 **B**- Biofilm assay showing the biofilm formation ability of STM after 72h of inoculation in
1050 presence of OS culture supernatant at high temperature conditions. Data is representative of
1051 N=4, n=4. One-way ANOVA is used to obtain the p-values. Statistical test is performed with
1052 respect to STM.

1053 **C-** Biofilm assay showing the biofilm formation ability of STM after 72h of inoculation in
1054 presence of OS culture supernatant under Proteinase K treatment. Data is representative of
1055 N=4, n=4. One-way ANOVA is used to obtain the p-values. Statistical test is performed with
1056 respect to STM.

1057

1058 **D**- Coomassie-stained SDS-PAGE demonstrating the size range of the differential protein
1059 bands present in OS supernatant as opposed to the tryptic soy broth media control.

1060 **E**- Biofilm assay showing the biofilm formation ability of STM after 72h of inoculation in
1061 presence of varying concentration OS culture supernatant. Data is representative of N=4, n=4.
1062 One-way ANOVA is used to obtain the p-values. Statistical test is performed with respect to
1063 STM.

1064 **F**- Biofilm assay showing the biofilm formation ability of STM after 72h of inoculation in
1065 presence of OS culture supernatant fractions fractionated using 3kDa Amicon filter. Data is
1066 representative of N=4, n=4. One-way ANOVA is used to obtain the p-values. Statistical test is
1067 performed with respect to STM.

G- Biofilm assay showing the biofilm formation ability of STM after 72h of inoculation in presence of OS culture supernatant fractions fractionated using 10kDa Amicon filter. Data is representative of N=4, n=4. One-way ANOVA is used to obtain the p-values. Statistical test is performed with respect to STM.

H- Summary table demonstrating the conditions tested for active molecule characterization and their effective outcome.

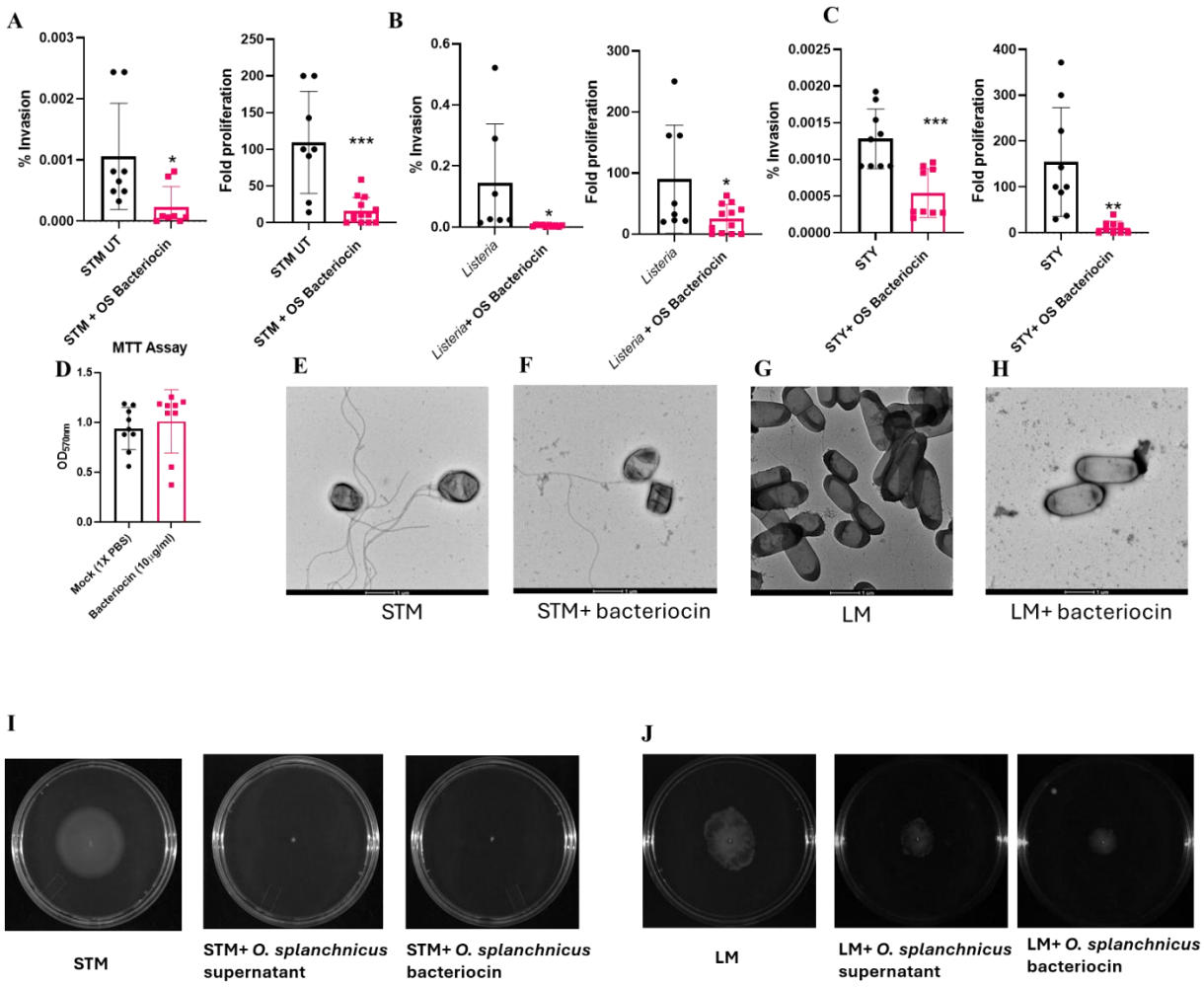

Fig. 9- *O. splanchnicus* bacteriocin restricts both *Salmonella* and *Listeria* pathogenesis *in vitro*

1079 **A**- Percent invasion and intracellular fold proliferation of STM in Caco-2 cells under OS
1080 bacteriocin (10µg/ml) treatment. Data is representative of N=2, n=3. Unpaired t-test is used to
1081 obtain the p-values.

1082 **B**- Percent invasion and intracellular fold proliferation of LM in Caco-2 cells under OS
1083 bacteriocin (10µg/ml) treatment. Data is representative of N=2, n=3. Unpaired t-test is used to
1084 obtain the p-values.

1085 **C**- Percent invasion and intracellular fold proliferation of STY in Caco-2 cells under OS
1086 bacteriocin (10µg/ml) treatment. Data is representative of N=2, n=3. Unpaired t-test is used to
1087 obtain the p-values.

1088 **D**-MTT assay evaluating the viability of Caco-2 cells upon 16h of mock or bacteriocin
1089 (10µg/ml) treatment. Data is representative of N=2, n=4.

1090 **E-F**-TEM images of STM under untreated (D) or bacteriocin (10µg/ml) (E) treatment to assess
1091 the possession of flagella.

1092 **G-H**- TEM images of LM under untreated (D) or bacteriocin (10µg/ml) (E) treatment to assess
1093 the possession of flagella.

1094 **I-** Swimming motility assay of STM under OS supernatant or bacteriocin treatment.

1095 **J**- Swimming motility assay of LM under OS supernatant or bacteriocin treatment.

1096

GRAPHICAL ABSTRACT

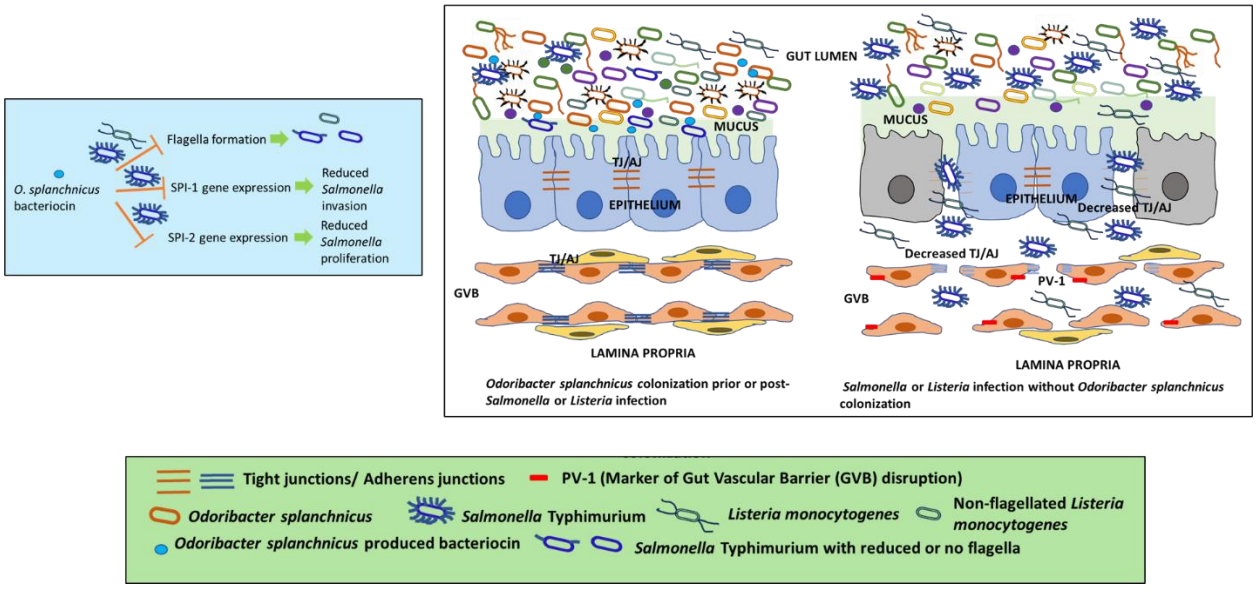

SUPPLEMENTARY FIGURES AND LEGENDS

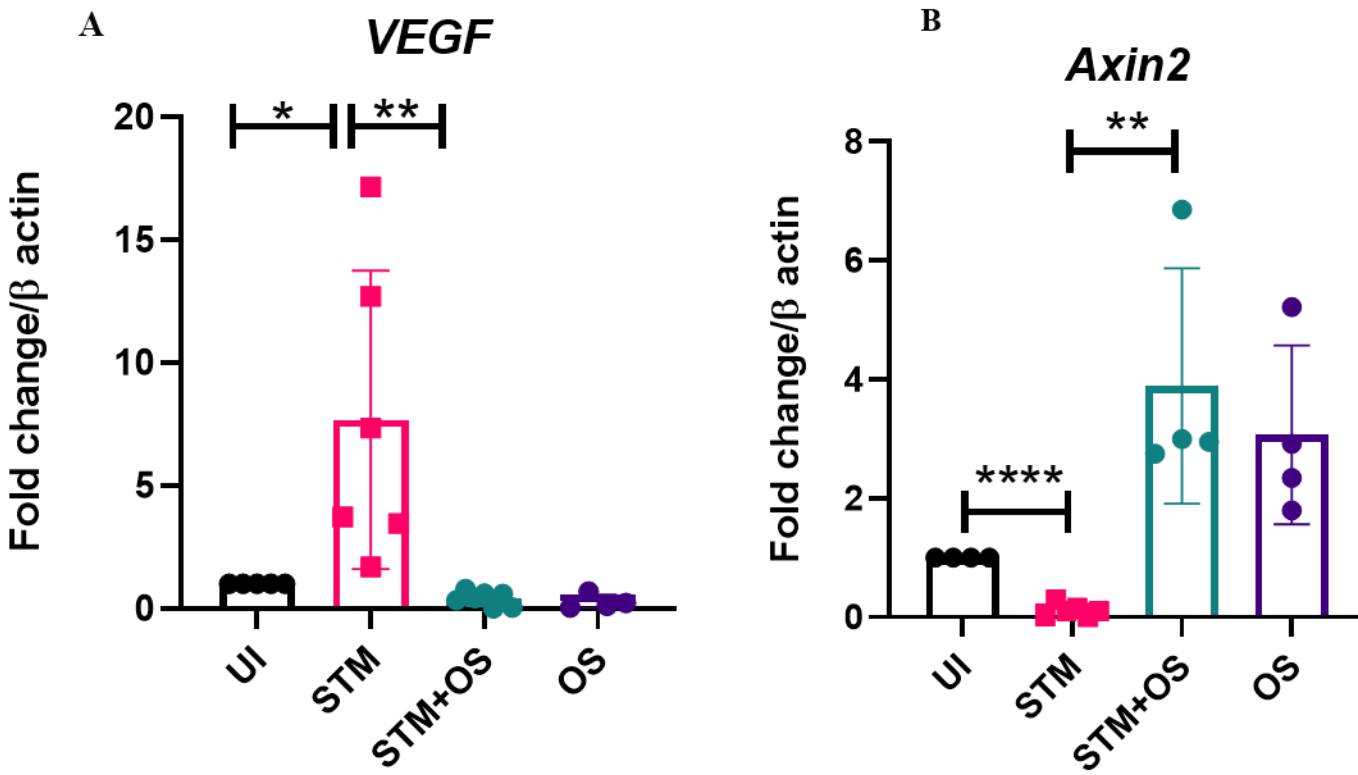

1102

1103

1104 **Fig S1. *O. splanchnicus* gut colonization prevents *Salmonella* dissemination by restricting**

1105 **intestinal GVB damage and angiogenesis**

1106 **A**- qPCR mediated gene expression of pro-angiogenic marker *Vegf* in STM-infected mice liver

1107 tissues in presence or absence of OS pre-colonization. Data is representative of N=2, n=4. Un-

1108 paired t-test was used to obtain the p-values.

1109 **B**- qPCR mediated gene expression of *Axin2* in STM-infected mice intestinal tissues in the

1110 presence or absence of OS pre-colonization. Data is representative of N=2, n=4. Un-paired t-

1111 test was used to obtain the p-values.

1112

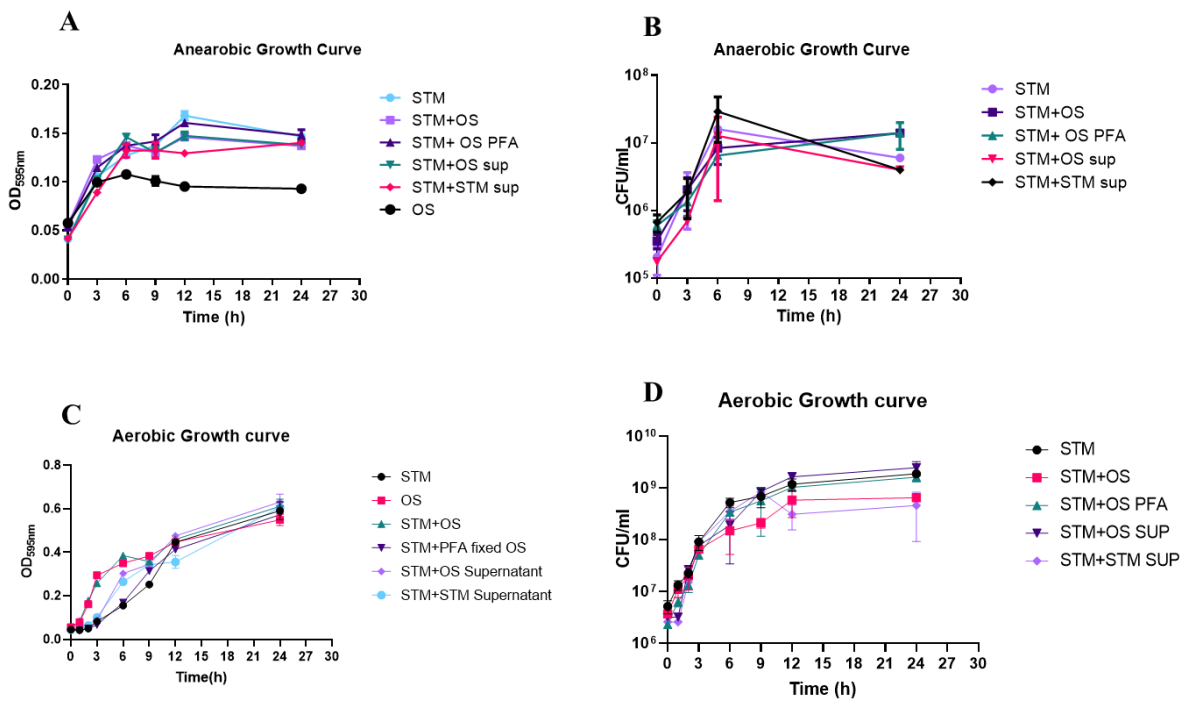

Fig. S2 In vitro growth kinetics of *Salmonella* Typhimurium in presence of live or dead *O. splanchnicus* or its culture supernatant

A-B Growth kinetics of STM-WT, OS, STM-WT in presence of OS, STM-WT in presence of STM or OS culture supernatant and STM-WT in presence of PFA-fixed OS in LB under anaerobic growth conditions.

C-D- Growth kinetics of STM-WT, OS, STM-WT in presence of OS, STM-WT in presence of STM or OS culture supernatant, STM-WT supernatant, and STM-WT in presence of PFA-fixed OS in LB under aerobic growth conditions.

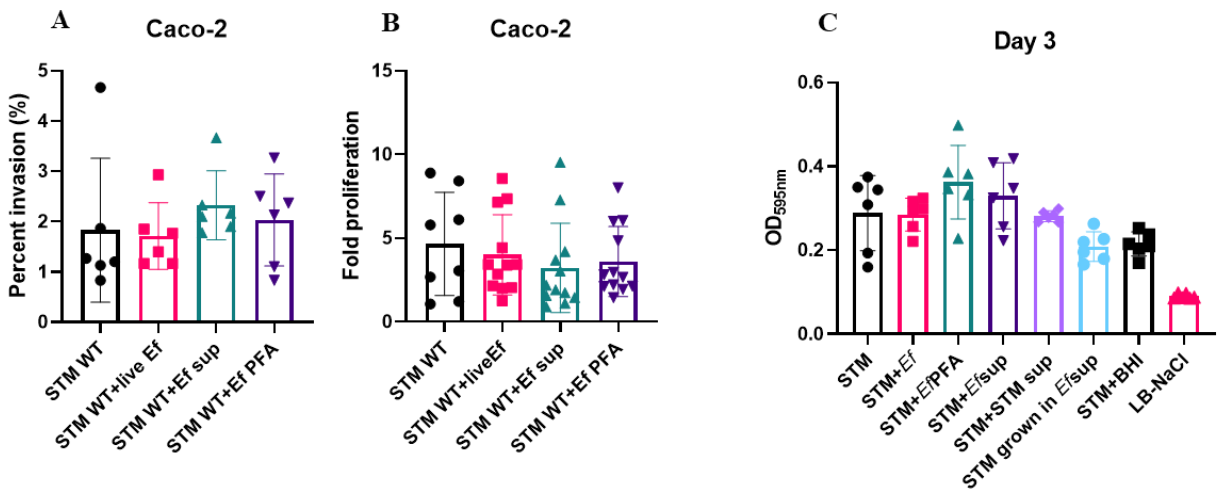

Fig S3. Unlike *O. splanchnicus, E. faecalis* fail to exert any inhibitory effect on *Salmonella in vitro* biofilm formation or *Salmonella* invasion and intracellular replication in human intestinal cells

A-Percent invasion of STM in Caco-2 cells in presence or absence of live *E. faecalis* (Ef), Ef culture supernatant, PFA-fixed-Ef. Data is representative of N=3, n=3. One-way ANOVA is used to obtain the p-values.

B-Intracellular proliferation of STM in Caco-2 cells in presence or absence of live Ef, Ef culture supernatant, PFA-fixed-Ef. Data is representative of N=3, n=3. One-way ANOVA is used to obtain the p-values.

C- Biofilm assay depicting the biofilm formation ability of STM-WT or STM-WT grown in Ef supernatant after 72h of inoculation in presence or absence of live Ef, Ef or STM culture supernatant, PFA-fixed. Crystal-violet staining was performed to assess the biofilm formation on the solid-liquid interphase and the $[OD]_{595}$ absorbance reading was recorded. Data is representative of N=3, n=3. One-way Anova is used to obtain the p-values.

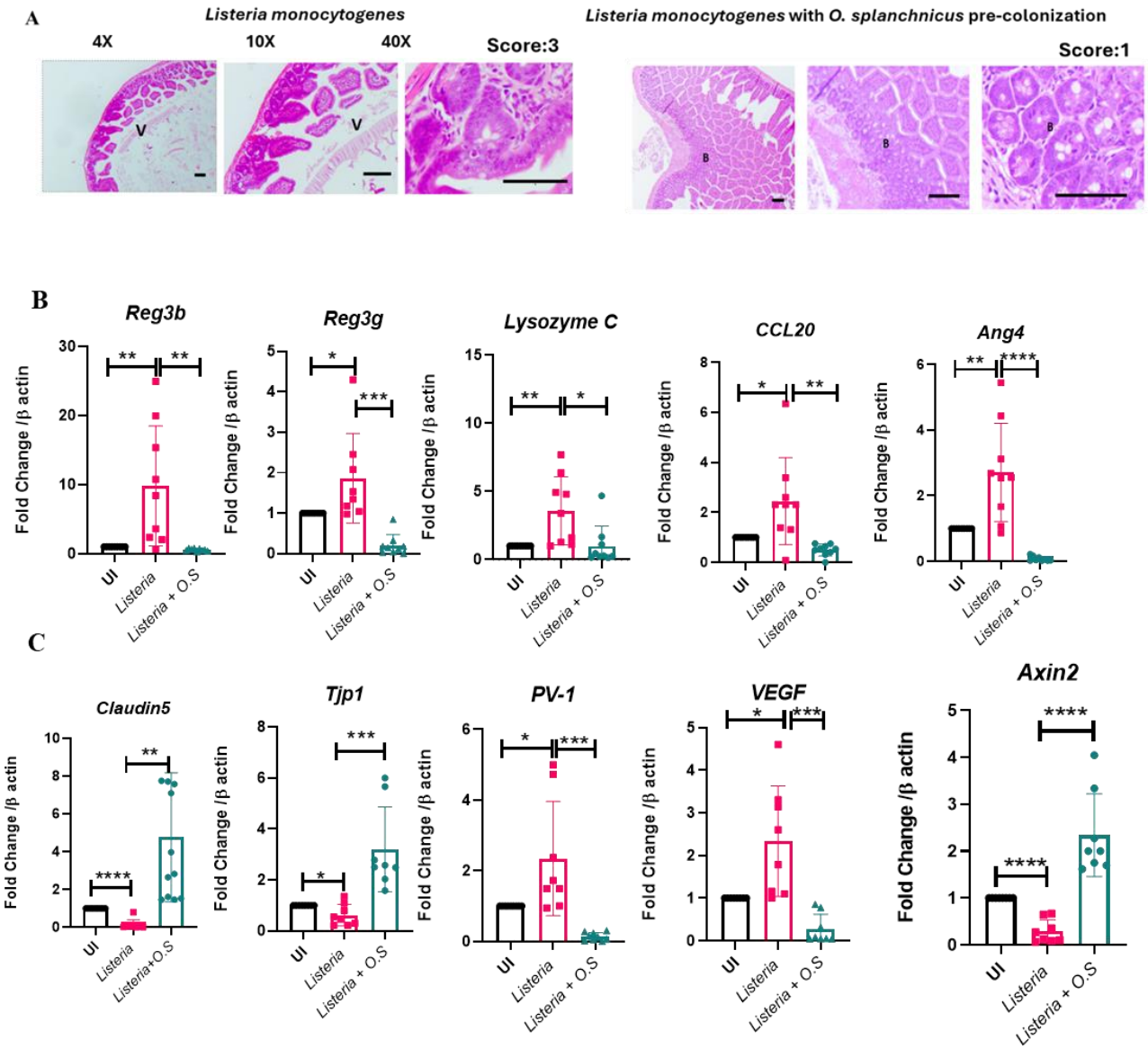
A
Listeria monocytogenes
4X
10X
40X
Score:3
V
Listeria monocytogenes with O. splanchnicus pre-colonization
Score:1
B
B
B
B
Reg3b
Reg3g
Lysozyme C
CCL20
Ang4
Fold Change /β actin
UI
Listeria
Listeria + O.S
C
Claudin5
Tjp1
PV-1
VEGF
Axin2
Listeria+O.S

1139

1140

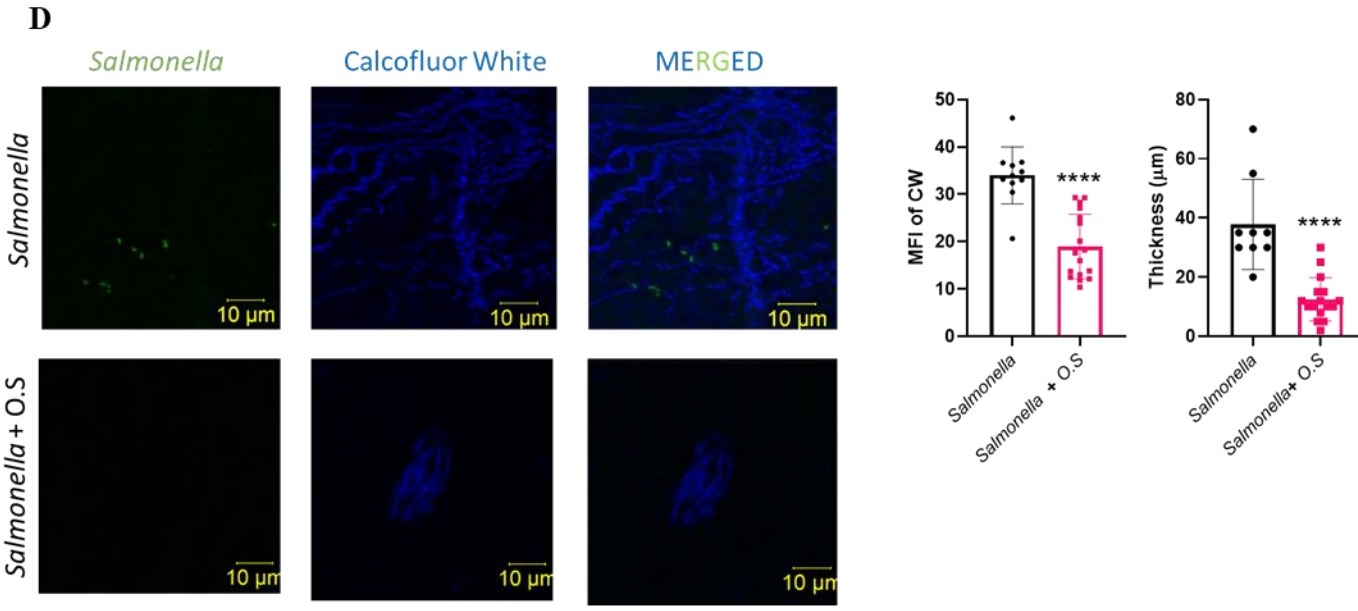
D
Salmonella
Calcofluor White
MERGED
Salmonella
Salmonella + O.S
10 µm
MFI of CW
Thickness (µm)
****
Salmonella
Salmonella + O.S

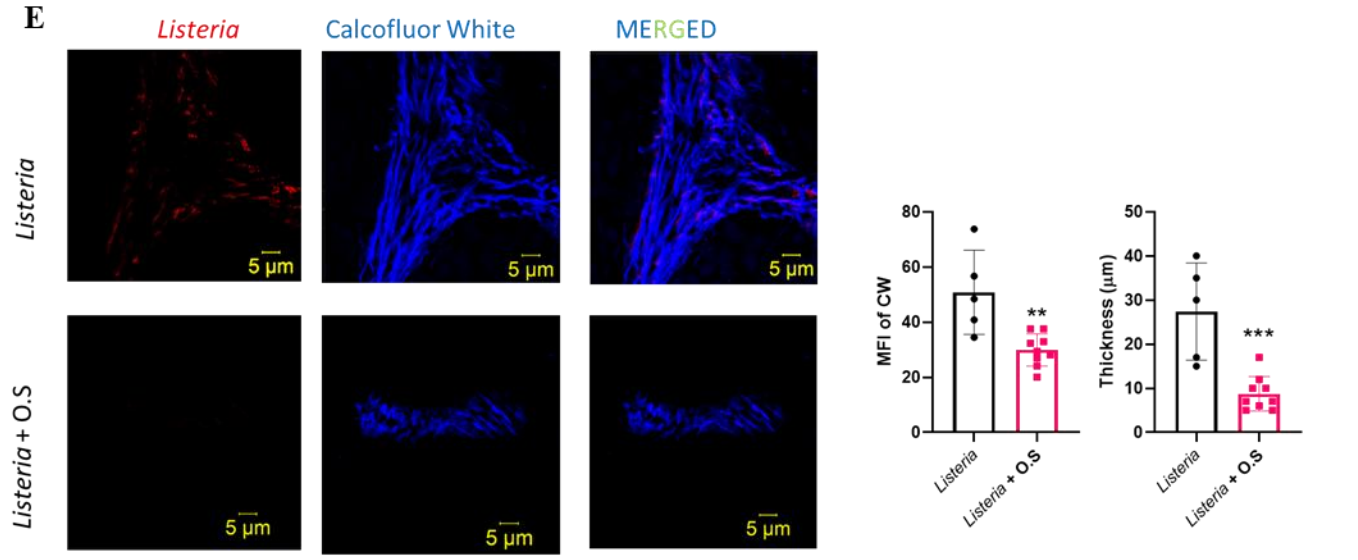
E
Listeria
Calcofluor White
MERGED
Listeria
Listeria + O.S
5 µm
MFI of CW
Thickness (µm)
**
***
Listeria
Listeria + O.S

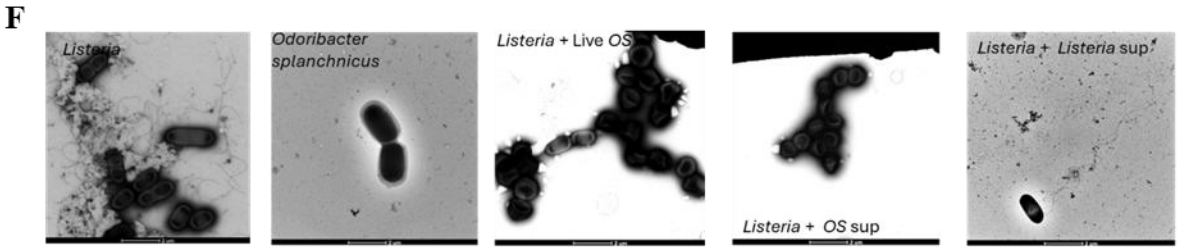
F
Listeria
Odoribacter splanchnicus
Listeria + Live OS
Listeria + OS sup
Listeria + Listeria sup

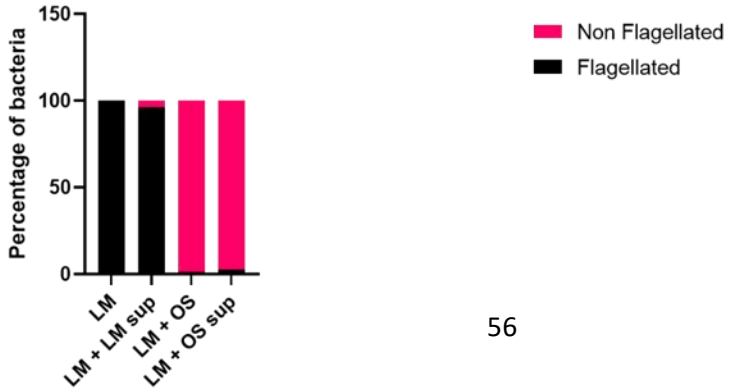
Percentage of bacteria
Non Flagellated
Flagellated
LM
LM + LM sup
LM + OS
LM + OS sup

1141

1142

1143 **Fig. S4. *Odoribacter splanchnicus* gut colonization protects mice against *Listeria***
1144 ***monocytogenes* pathogenesis similar to *Salmonella* infection**

1145 **A**-Haematoxylin-eosin-stained intestinal sections harvested from OS non-colonized or
1146 colonized mice cohorts at 5th-day-post-LM-infection. 0-represents normal pathology, 1-
1147 represents- mild pathology, 2-3-represents severe pathology.

1148 **B**-Quantitative gene expression data of several antimicrobial peptides (AMPs) precursor genes
1149 in LM-infected mice intestinal tissues harvested at 5th day post-infection from OS colonized or
1150 non-colonized cohorts. Unpaired Student's t-test is performed to obtain the p-values. Data is
1151 representative of N=2, n=9.

1152 **C**- Quantitative gene expression study of tight junction protein genes *Tjp1*, *Claudin5*, GVB
1153 damage marker *PV-1*, angiogenesis marker-*Vegf,* and *Axin2* in LM- infected mice intestinal
1154 tissues harvested at 5th-dpi from OS colonized or non-colonized cohorts. Unpaired Student's
1155 t-test is performed to obtain the p-values. Data is representative of N=2, n=5.

1156 **D-**Representative Calcofluor white (CW) staining of STM-infected mice spleen tissues at 5th-
1157 dpi. Data is representative of N=2, n=8 (tissue samples). Un-paired t-test was used to obtain
1158 the p-values.

1159 **E**- Representative CW staining of LM-infected mice spleen tissues at 5th-dpi. Data is
1160 representative of N=2, n=8 (tissue samples). Un-paired t-test was used to obtain the p-values.

1161 **F**- Transmission Electron Microscopic (TEM) images of LM in presence or absence of LM
1162 supernatant, OS and its supernatant to assess the possession of flagella. The quantification plot
1163 exhibits the percentage of bacterial flagellated or non-flagellated cells (number of cells
1164 quantified n$\geq$ 100)

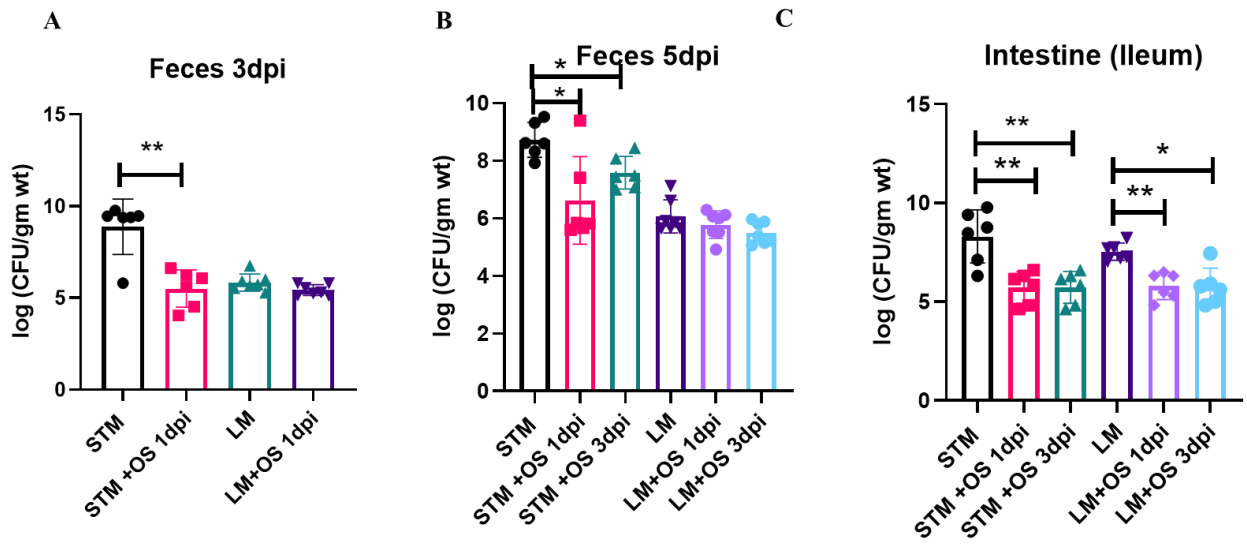

1165

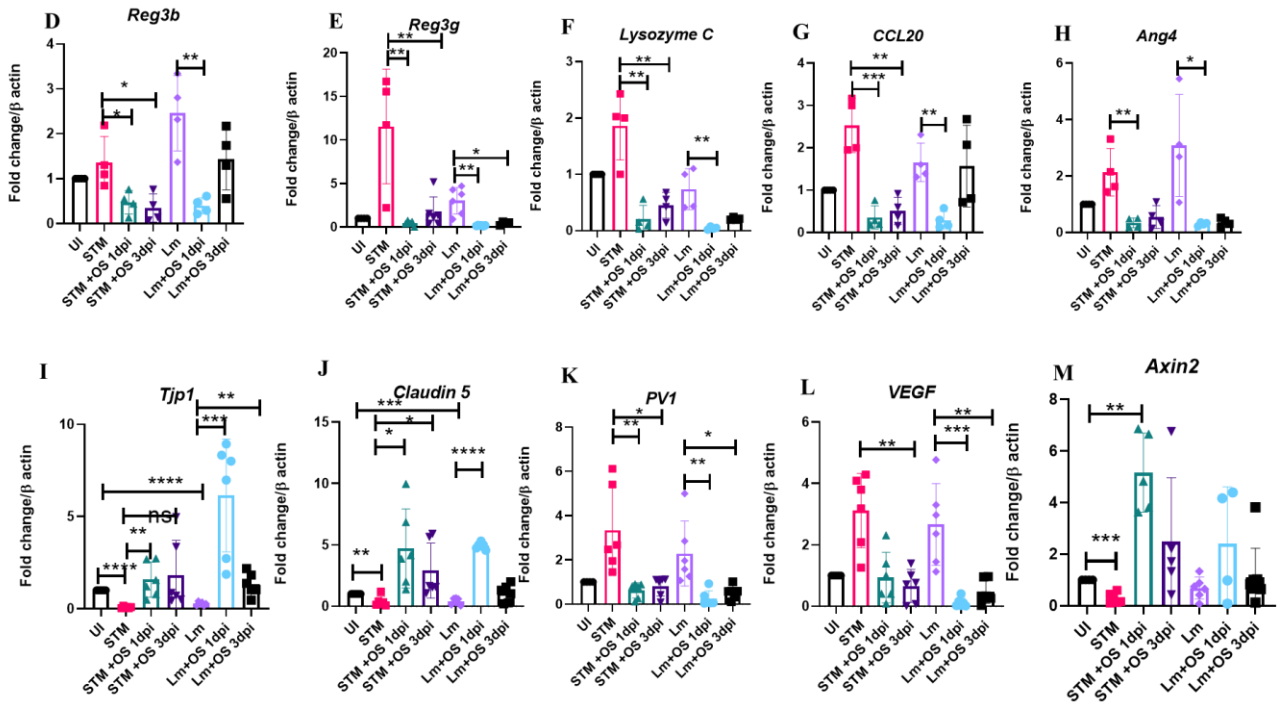

1166

1167

1168

1169

1170

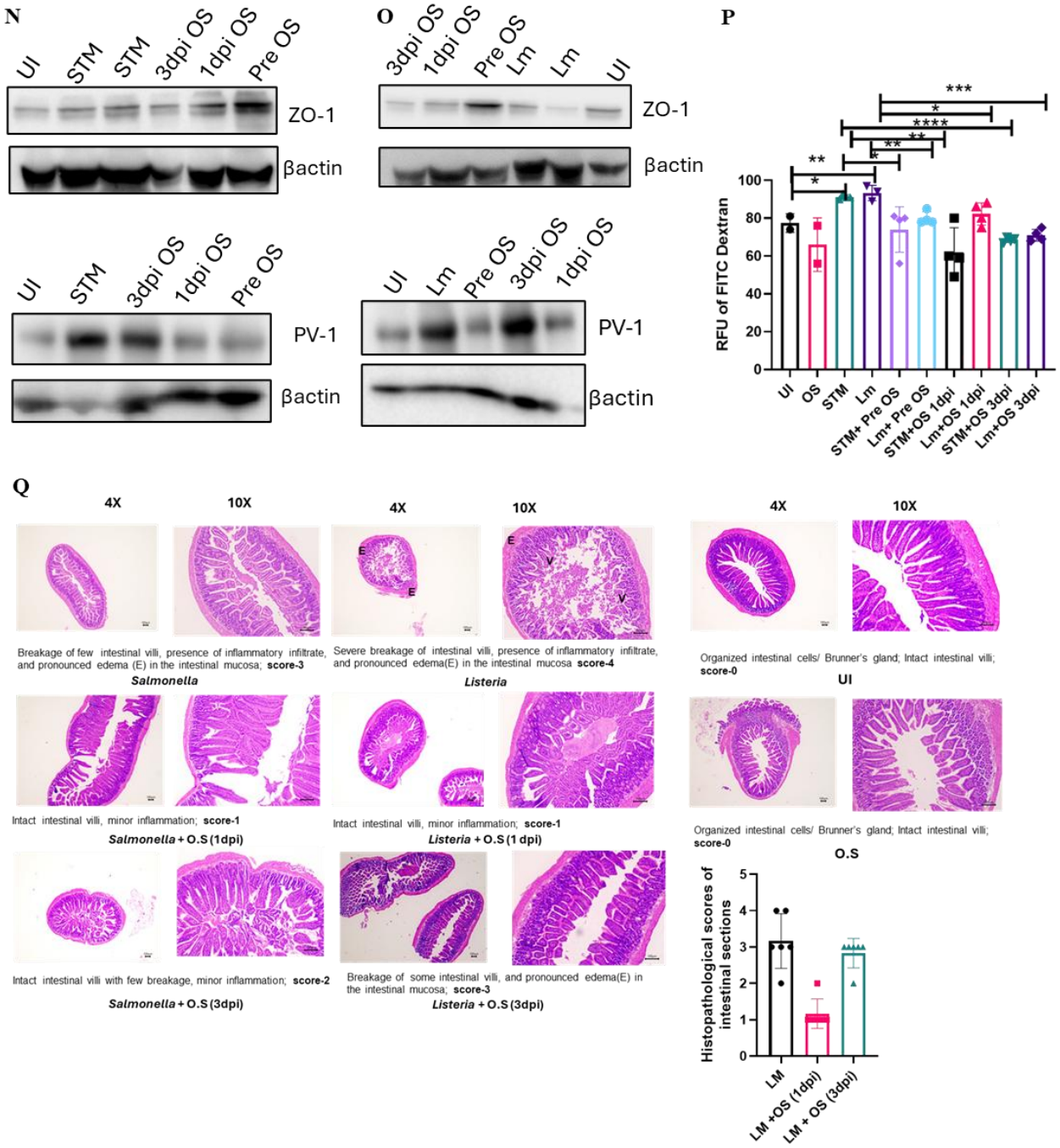
N
UI
STM
STM
3dpi OS
1dpi OS
Pre OS
ZO-1
βactin
UI
STM
3dpi OS
1dpi OS
Pre OS
PV-1
βactin
O
3dpi OS
1dpi OS
Pre OS
Lm
Lm
UI
ZO-1
βactin
UI
Lm
Pre OS
3dpi OS
1dpi OS
PV-1
βactin
P
RFU of FITC Dextran
UI
OS
STM
Lm
STM+ Pre OS
Lm+ Pre OS
STM+OS 1dpi
Lm+OS 1dpi
STM+OS 3dpi
Lm+OS 3dpi
Q
4X
10X
Breakage of few intestinal villi, presence of inflammatory infiltrate, and pronounced edema (E) in the intestinal mucosa; score-3
Salmonella
Severe breakage of intestinal villi, presence of inflammatory infiltrate, and pronounced edema(E) in the intestinal mucosa score-4
Listeria
Organized intestinal cells/ Brunner's gland; Intact intestinal villi; score-0
UI
Intact intestinal villi, minor inflammation; score-1
Salmonella + O.S (1dpi)
Intact intestinal villi, minor inflammation; score-1
Listeria + O.S (1 dpi)
Organized intestinal cells/ Brunner's gland; Intact intestinal villi; score-0
O.S
Intact intestinal villi with few breakage, minor inflammation; score-2
Salmonella + O.S (3dpi)
Breakage of some intestinal villi, and pronounced edema(E) in the intestinal mucosa; score-3
Listeria + O.S (3dpi)
Histopathological scores of intestinal sections
LM
LM +OS (1dpi)
LM + OS (3dpi)

1171

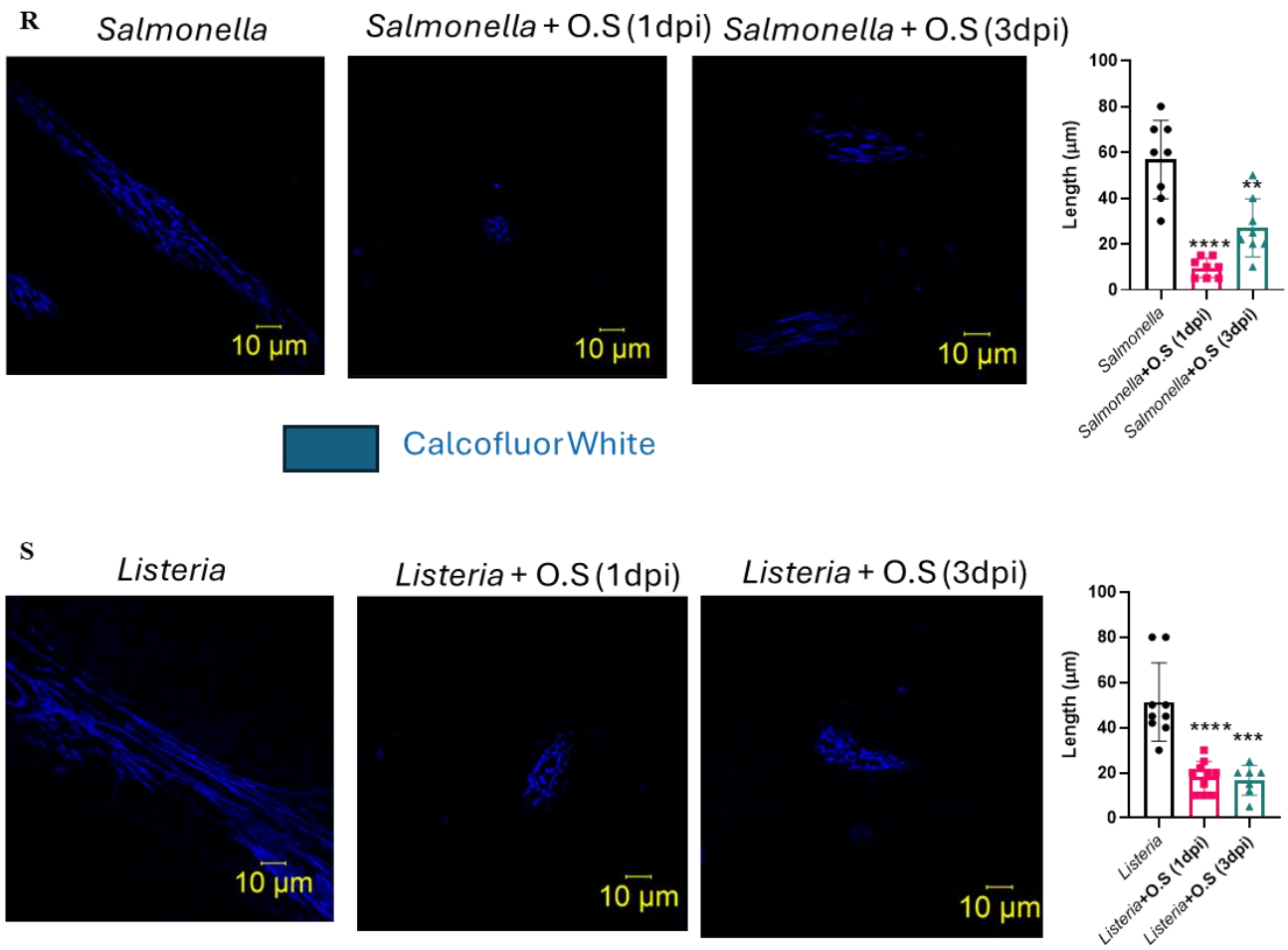

Fig. S5 *Odoribacter splanchnicus* administration post-establishment of infection protected mice against *Listeria monocytogenes* and *Salmonella* Typhimurium

A-C- STM and LM organ loads in feces at 3rd day post-infection (A), 5th post-infection (B) and in ileal tissues (contents and wall) at 5th day post-infection (C) upon OS administration at 1-dpi or 3-dpi. Data is representative of N=2, n=6 where N denotes number of biological replicates and n denotes the number of mice per group. Mann-Whitney Test was performed to obtain p-values.

D-H-Quantitative gene expression data of several antimicrobial peptides (AMPs) precursor genes in LM and STM-infected mice intestinal tissues harvested at 5th dpi upon OS colonization

1183 at 1-dpi or 3-dpi. Unpaired Student's t-test is performed to obtain the p-values. Data is
1184 representative of N=2, n=4.

1185 **I-M**- Quantitative gene expression study of tight junction protein genes *Tjp1*, *Claudin5*, GVB
1186 damage marker *PV-1*, angiogenesis marker-*Vegf,* and *Axin2* in LM and STM-infected mice
1187 intestinal tissues harvested at 5th-dpi upon OS colonization at 1-dpi or 3-dpi. Unpaired
1188 Student's t-test is performed to obtain the p-values. Data is representative of N=2, n=6.

1189 **N-O**- Immunoblotting representing the protein expression profile of ZO-1, and PV-1 in
1190 *Salmonella* (N) or *Listeria* (O)-infected mice intestinal tissue harvested on 5th-dpi with or
1191 without OS pre-or post-colonization (1-dpi or 3-dpi). Data is representative of N=3.

1192 **P**- Estimation of FITC fluorescence in mice plasma via gut permeability assay in *Salmonella*
1193 or *Listeria*-infected mice cohorts with or without OS pre-or post-colonization (1dpi or 3dpi)
1194 upon oral administration of FITC Dextran (25mg/kg) 4h before euthanization at 5th-dpi.
1195 Unpaired Student's t-test is performed to obtain the p-values. Data is representative of N=2,
1196 n=4 (UI and OS, n=2).

1197 **Q-** Haematoxylin-eosin-stained intestinal sections harvested at 5th-dpi from Uninfected (UI) or
1198 *Salmonella* or *Listeria*-infected mice cohorts having non-administered or administered OS (at
1199 1st or 3rd dpi). 0-represents normal pathology, 1- represents- mild pathology, 2-3-represents
1200 severe pathology. Data is representative of N=2, n=6.

1201 **R**- Representative Calcofluor white (CW) staining of STM-infected mice spleen tissues at 5th-
1202 day post-infection with or without OS administration at 1st or 3rd dpi depicting the
1203 quantification of the length of the fibril architecture of CW-stained sections. One-way ANOVA
1204 and multiple comparison test were used to obtain the p-values.

1205 **S**- Representative CW staining of LM-infected mice spleen tissues at 5th-dpi with or without
1206 OS administration at 1st or 3rd dpi depicting the quantification of the length of the fibril

architecture of CW-stained sections. One-way ANOVA and multiple comparison test were used to obtain the p-values.

A

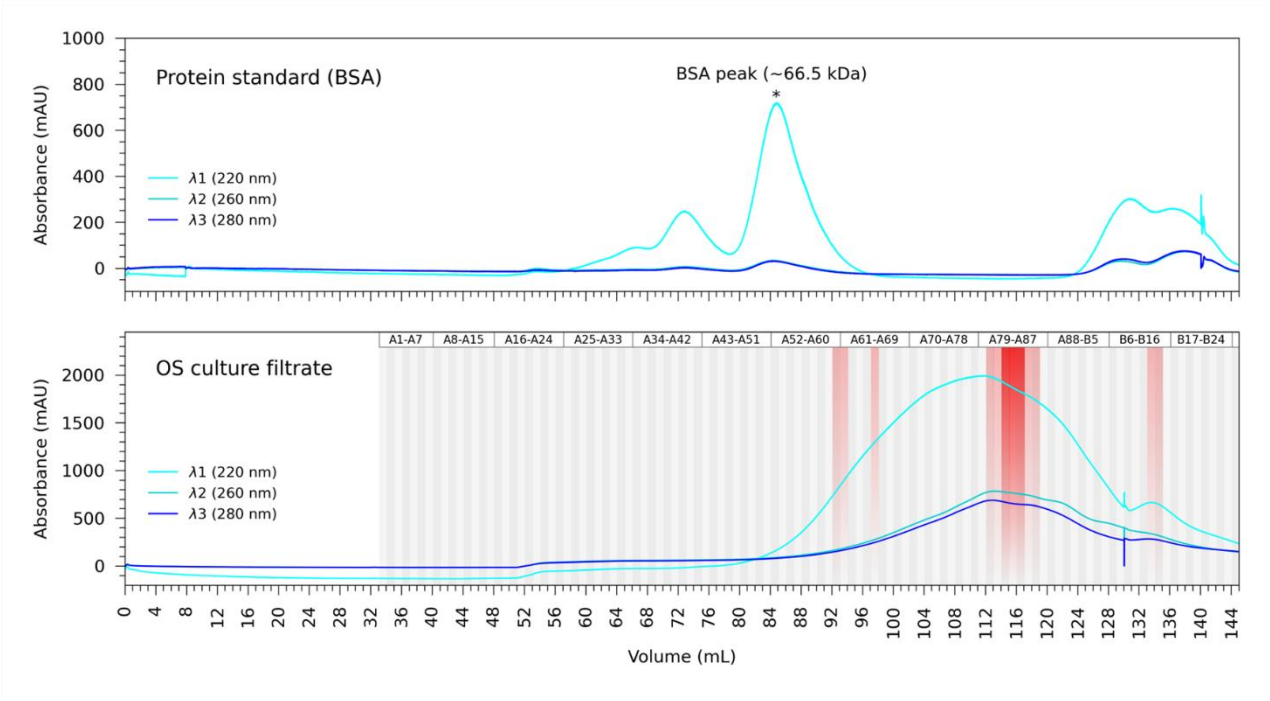

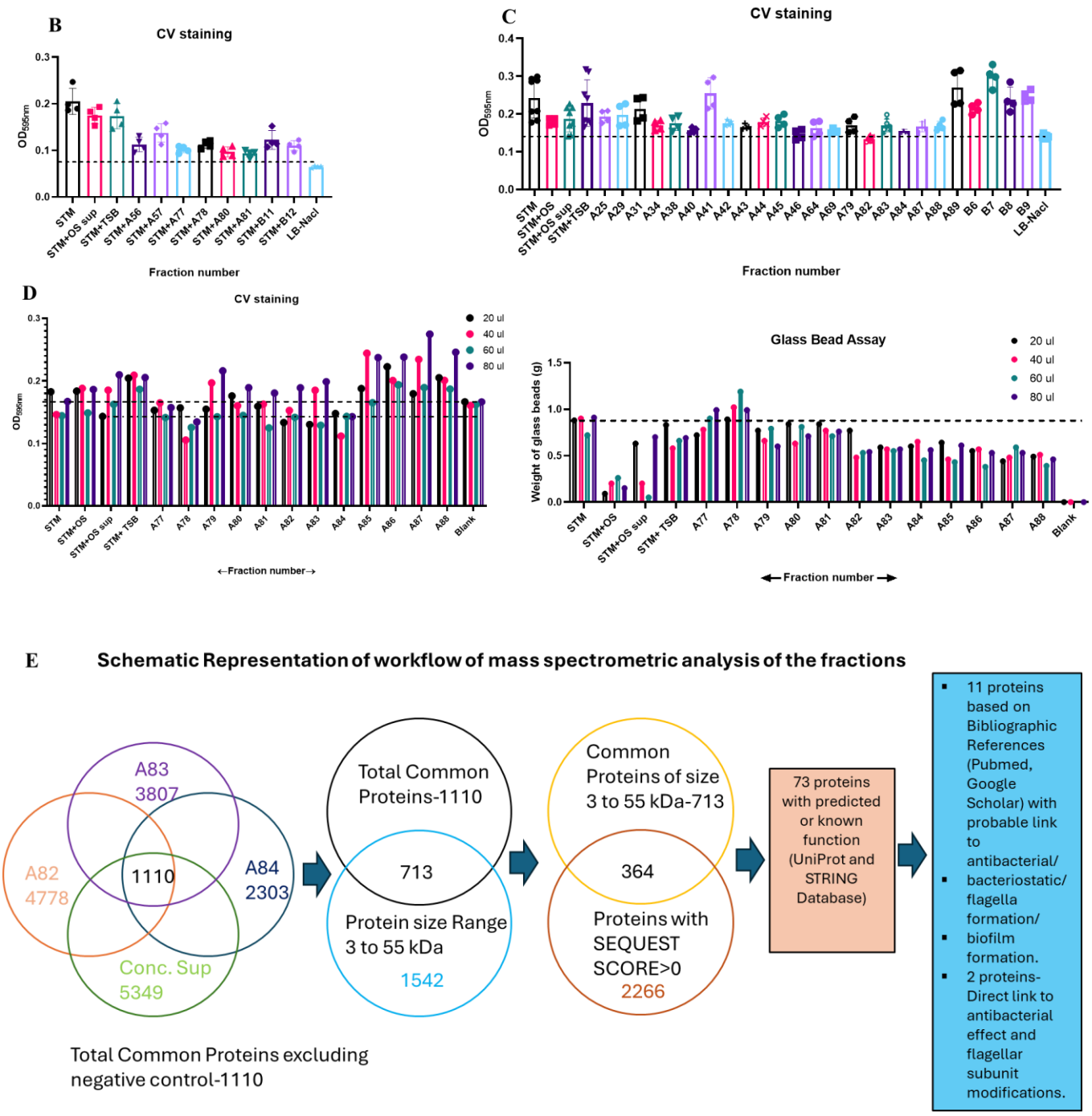

Fig. S6 Characterization of the inhibitory active molecule within *O. splanchnicus* culture supernatant

A-Gel filtration chromatogram of protein standards and the OS culture supernatant. Red shaded region shows the fractions with biofilm inhibitory activity. The dark shaded region indicates the fractions with the highest inhibitory activity.

1219 **B-C**- Biofilm assay showing the biofilm formation ability of STM after 72h of inoculation in
1220 presence of OS supernatant gel filtration fractions. Data is representative of N=2, n=2. One-
1221 way ANOVA is used to obtain the p-values.

1222 **D**- Biofilm assay showing the biofilm formation ability of STM after 72h of inoculation in
1223 presence of varying concentration of OS supernatant biofilm inhibitory gel filtration fractions.
1224 Data is representative of N=2, n=1.

1225 **E**-Schematic representation of the workflow of mass spectrometric analysis of the gel filtration
1226 fractions (A82, A83, A84 and Concentrated supernatant).

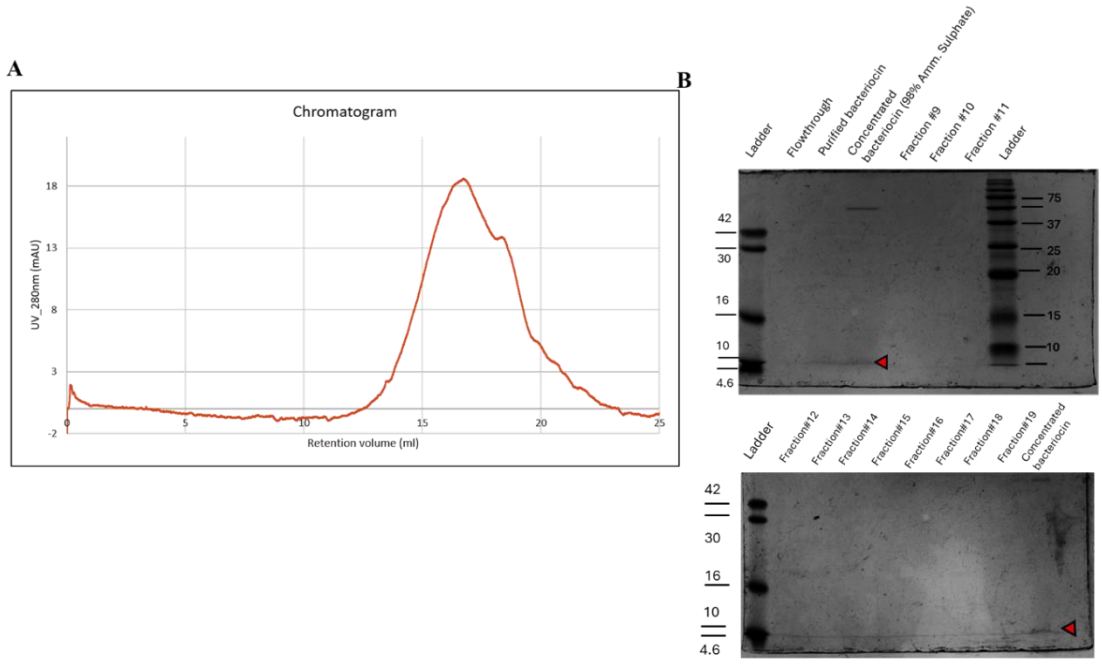

1227

1228 **Fig. S7 Purification procedure of *O. splanchnicus* produced bacteriocin via ammonium**
1229 **sulphate precipitation method followed by Fast Performance Liquid Chromatography**

1230 **A**-Size exclusion chromatogram of OS-produced bacteriocin fractions post 95-98%
1231 ammonium sulphate precipitation.

1232 **B**- Coomassie-stained SDS PAGE showing the purified and concentrated OS bacteriocin.

1233

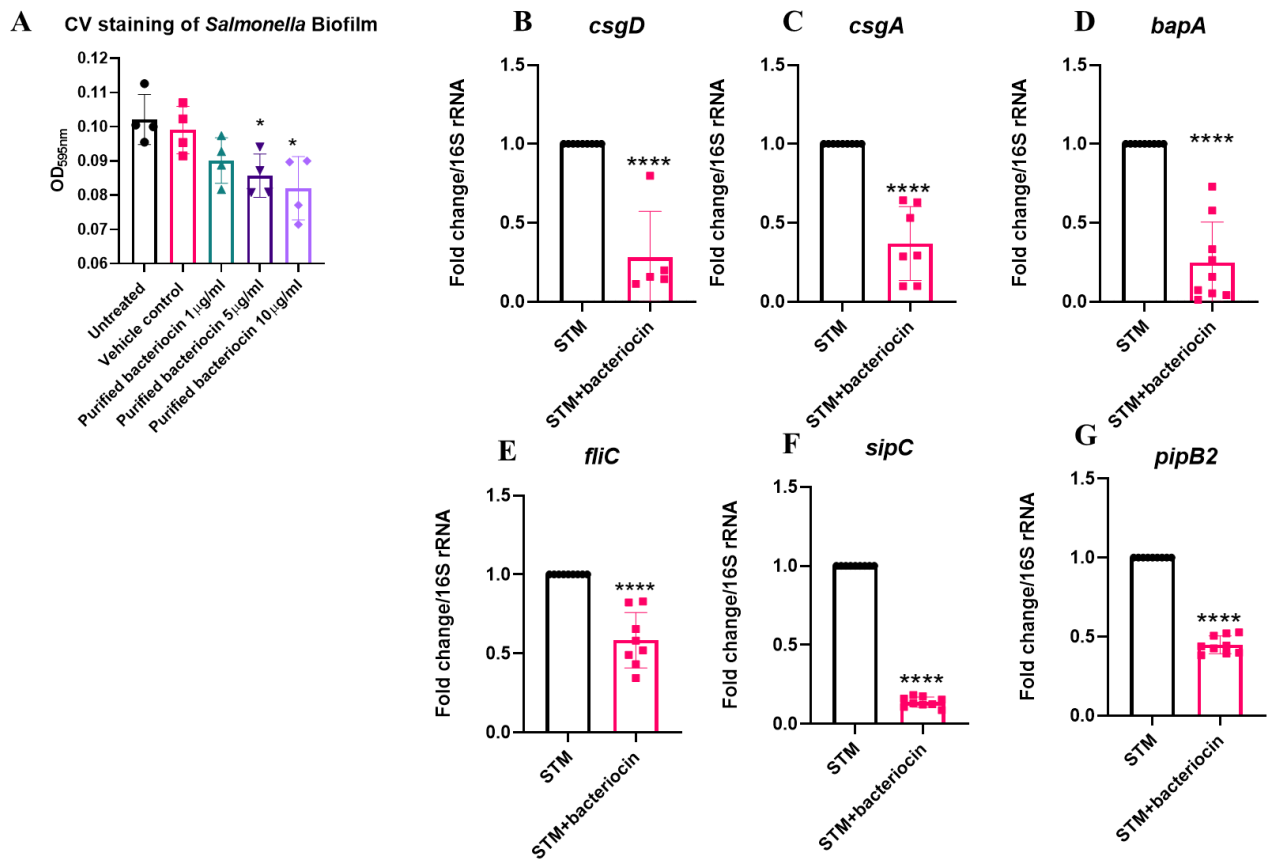

1234

1235 **Fig. S8 *O. splanchnicus* bacteriocin attenuates *Salmonella* pathogenesis *in vitro***

1236 **A**- Biofilm assay showing the biofilm formation ability of STM after 72h of inoculation under

1237 varying concentration of OS bacteriocin. Data is representative of N=2, n=2. Unpaired t-test is

1238 used to obtain the p-values.

1239 **B-G**- RT-qPCR mediated gene expression of STM biofilm regulatory genes *csgD* (B),

1240 *csgA*(C), *bap* (D), along with flagellar gene *fliC*(E), SPI-1-*sipC* (F) and SPI-2-*pipB2*(G) in

1241 presence or absence of OS bacteriocin treatment. Data is representative of N=2, n≥5. Unpaired

1242 Student's t-test was used to obtain the p-values.

1243

1244

1245

1246 **Table S1- Selected List of 11 proteins from Mass Spectrometric Analysis based on**

1247 **bibliographic search**

Accession ID	Protein Name and	Referenced Function
A0A412WBT8	Immunity protein Imm5 domain-containing protein	Uncharacterized
F9Z8G5	Peptidase	Modulate biofilm formation and host defense.
R6F650	Carboxyl-terminal protease	Critical for post-translational processing and associated with regulation of gene expression, stress response, maintenance of cell envelope integrity and bacterial virulence.
A0A412TJE3	ATP-dependent Clp protease proteolytic subunit	Influence virulence and infectivity of pathogenic bacteria. ClpP enhance biofilm formation in *Enterococcus faecalis*.
F9Z604	Peptidase C39 bacteriocin processing	The cysteine peptidase cleave the double glycine leader peptides from the precursors of bacteriocin
A0A412TJV3	UDP-2,4-diacetamido-2,4, 6-trideoxy-beta-L-altropyranose hydrolase	It catalyzes the third step in the biosynthesis of pseudaminic acid. Pseudaminic acid is a sialic-like sugar that modifies flagellin.
A0A412WSU3	Bacteriocin	Antimicrobial peptides that can kill or inhibit closely related or unrelated bacterial strains.
A0A413I832	Serine Protease	Extracellular proteases regulate biofilm formation and growth of competitors.
A0A412W3J2	Glutamate dehydrogenase	Involved in bacterial response to stress adaptation and virulence.
A0A412WSS0	Bacteriocin	Antimicrobial peptides that can kill or inhibit closely related or unrelated bacterial strains.
F9ZBU9	Peptidylprolyl isomerase	Promote biofilm formation in *Mycobacterium tuberculosis.*

1248

1249 **Table S2-List of primers**

Primer Name	Sequence (5'---3')
O. splanchnicus 16S rRNA FP	ATGTAATGATGAGCACTCTAACGG
O. splanchnicus 16S rRNA RP	GGCTTTTGAGATTGGCATCC
PV-1 FP	CGAACTGGAGGCGCGTAA
PV-1 RP	GCAGCGACTTGGCCTTGAC
Claudin5 FP	CCCAGTTAAGGCACGGGTAG
Claudin5 RP	GGCACCGTCGGATCATAGAA

βactin FP	CAGCAAGCAGGAGTACGATG
βactin RP	GCAGCTCAGTAACAGTCCG
Vegf FP	GCAGCGACAAGGCAGACTAT
Vegf RP	AACCTCCTCAAACCGTTGGC
Tjp1 FP	TCTTGCAAAGTATCCCTTCTGT
Tjp1 RP	CAGAAATCGTGCTGATGTGCC
Reg3b FP	GCTTGTCAAGAGCTTCTGGATTTC
Reg3b RP	TGTCCCTTGTCCATGATGCTC
Reg3g FP	CGCTGAAGCTTCCTTCCTGT
Reg3g RP	GGGTTCATAGCCCAGTGTCG
Lysozyme C FP	GGTCTACAATCGTTGTGAGTTG
Lysozyme C RP	TGAGCTAAACACACCCAGTCA
CCL 20 FP	GCAACTACGACTGTTGCCTC
CCL20 RP	TTCTTGACTCTTAGGCTGAGGA
Ang4 FP	TGGTTGTGATTCCTCCAACTCT
Ang4 RP	TGTTGACATCTTTGCAAGGCG
fliC FP	CTAAACAAACTGGGTGGCGC
fliC RP	GCACCCAGGTCAGAACGTAA
bapA FP	ACGGTGACTACGCCTAAAAC
bapA RP	CTTCCGCCTCAGTCACTTTT
csgD FP	ACGATTATCCCTACCGTGAA
csgD RP	GCGGACTCGGTGCTGTTGTA
Salmonella 16S rRNA FP	GTGAGGTAACGGCTCACCAA
Salmonella 16S rRNA RP	TAACCGCAACACCTTCCTCC

sipC FP	GCAGTACGCCGCTACTCAGG
sipC RP	AGCGCGAATATTGCCTGCGA
pipB2 FP	TGGCGCCAATTTACAACACGC
pipB2 RP	CTCGCCTTTCGCAGGTTTGC
csgA FP	TCGCAGCAATCGTAGTT
csgA RP	CGGAACCGTACTGATAA

1250

1251 **Table S3-List of Antibodies**

Antibody Name	**Catalogue Number**	**Source**
PV-1	**A15906-20ul (Abclonal)**	**Rabbit**
ZO-1	**R26.4C DHSB, CRL 1597**	**Mouse**
β actin	**A3854 (Sigma), Clone AC-15**	**Mouse**

1252

1253